Cherenkov detector for proton Flux Measurement (CpFM)

Leonid Burmistrov

on behalf of the UA9 Cherenkov detector team

UA9

[1] <u>L. Burmistrov</u>, [1] D. Breton, [1] V. Chaumat, [1] J. Colin, [3] G. Cavoto, [1] S. Conforti Di Lorenzo, [3] M. Garattini, [3] F. Iacoangeli, [1] J. Jeglot, [1] J. Maalmi, [2] S. Montesano, [1] V. Puill, [2] R. Rossi, [2] W. Scandale, [1] A. Stocchi, [1] J-F Vagnucci

[1] LAL, Univ Paris-Sud, CNRS/IN2P3, Orsay, France
[2] CERN - European Organization for Nuclear Research, CH-1211 Geneva 23, Switzerland
[3] INFN - Roma La Sapienza, Italy

CERN INFN CNRS IN2P3 Les deux infinis LAL Laboratoire de l'Accélérateur Linéaire SERDI Service d'Electronique, Recherche en Détecteurs et Instrumentation

Outline

1. Introduction

- Improvements of the collimation system at LHC
- UA9 experiment and charged particles in the bent crystal

2. CpFM detector

- CpFM detection chain components
- Geant4 simulation of the CpFM

3. Beam tests

- Beam tests at BTF Frascati.
- Results

4. Conclusion

Improvements of the collimation system at LHC

At LHC particles surrounding the beam core **(beam halo)** can be lost:

- → Damaging the accelerator
- → Distorting detector functioning

→ Luminosity limitation → Physics goals limitation

Present collimation at LHC

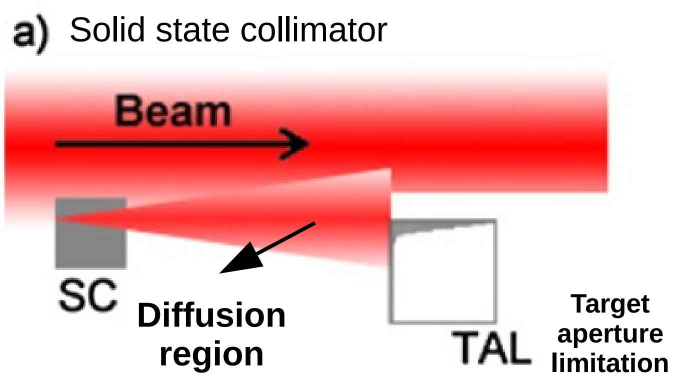

Multi-stage collimation systems to absorb this beam halo.

These systems are composed of massive collimators and absorbers very close to the beam.

Improved collimation at LHC

“Smart” collimation system

Direct the beam halo promptly onto secondary collimator

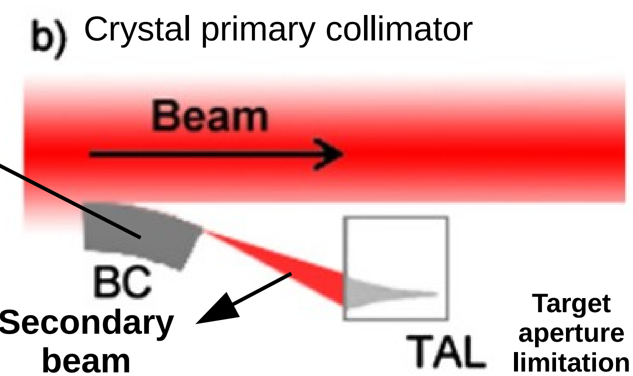

How to build “smart” collimator ?

Amorphous body (AB)

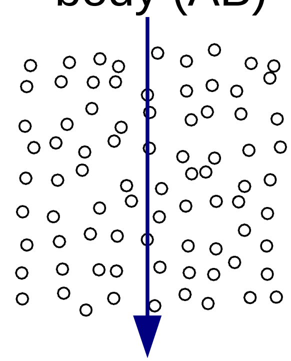

Interaction with right oriented crystal is smaller then with AB

↓

But how to deflect the beam with a crystal ?

↓

See next slide

Crystal

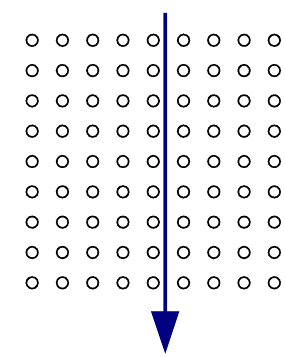

Crystal vs bent crystal

First idea by Tsyganov (1976)

Tsyganov E.N. Estimates of Cooling and Bending Processes for Charged Particle Penetration through a Monocrystal. Preprint No. TM 684. Batavia: Fermilab, 1976. 8 p.

If crystal planes are correctly oriented with respect to the incoming particle – it can be trapped via potential parabolic barrier between the lattices (**planar channeling effect**).

Crystal

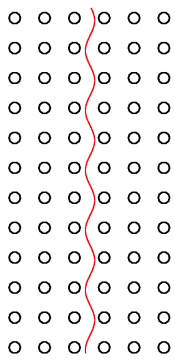

Mean continuum potential approximation

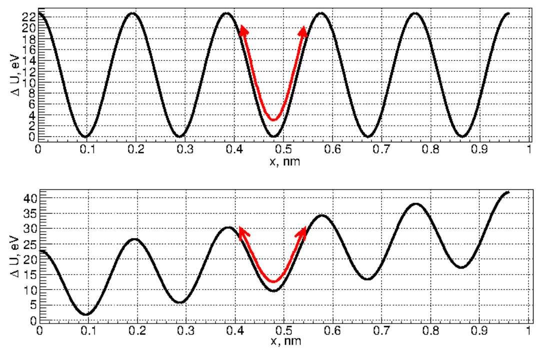

Bent crystal

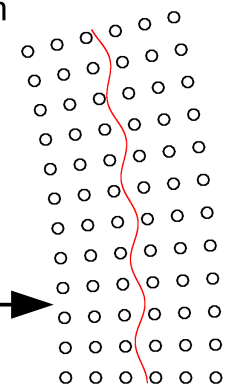

First observation (1979)

A.F. Elishev, et al. "Steering of charged particle trajectories by a bent crystal." Physics Letters B 88.3 (1979): 387-391.

Tests of the bent crystal as a primary collimator in the circular accelerator (SPS) since 2009 by **UA9 collaboration**.

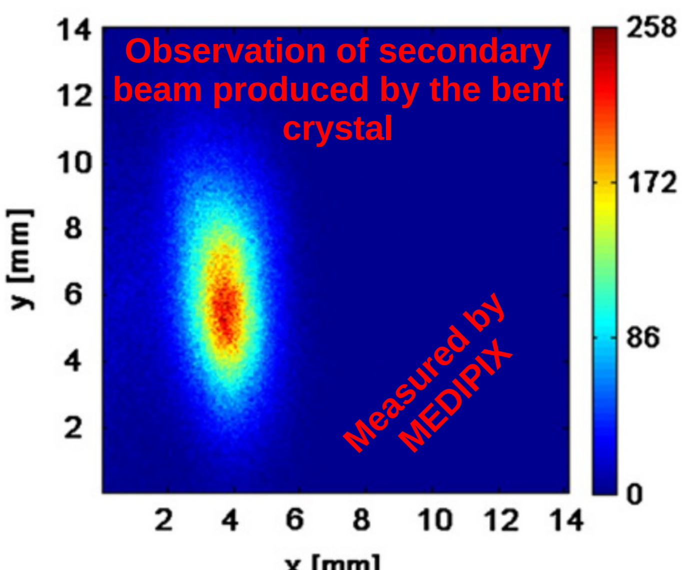

First results on the SPS beam collimation with bent crystals
(W. Scandale et al. Physics Letters B 692 (2010) 78–82)

↓

Final goal is to use "smart" collimator at LHC

↓

Additional device needed to monitoring the deflected beam

↓

CpFM

CpFM detection chain components

Cherenkov detector for proton Flux Measurements (CpFM)

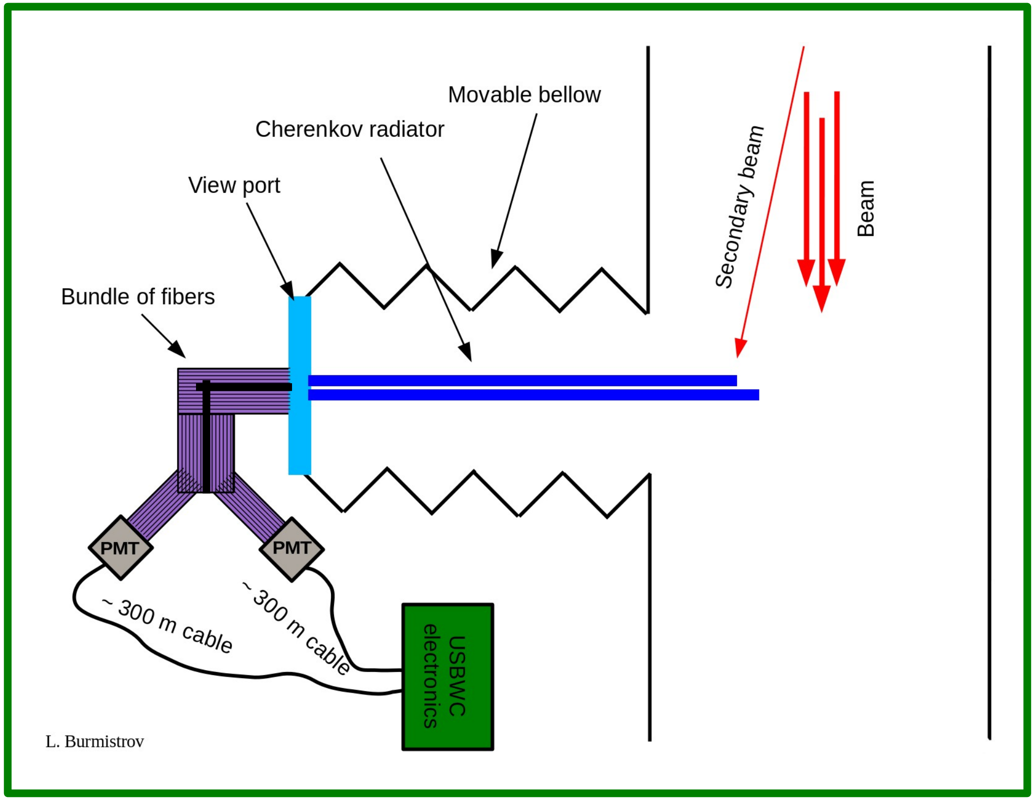

Main constrains for such device:

- Aim: **count the number of protons** with a precision of about **5 %** (100 incoming protons).
- No **degassing materials** (inside the primary vacuum).
- **Radiation hardness** of the detection chain (very hostile radioactive environment ~ 10 MGy)

- The Cherenkov light will propagate inside the **fused quartz* radiators**: one for beam monitoring and another for background measurements.
- The flange with quartz view port attached to the movable bellow.
- Quartz/quartz (core/cladding) radiation hard fibers 10 m long.
- Photo multiplier tube (PMT) situated away (~ 10 m) from the beam pipe with quartz window.
- 300 m low attenuation cable CKB50 (bringing signal to readout electronics)
- USB-WC electronics D. Breton et al. "USING ULTRA FAST ANALOG MEMORIES FOR FAST PHOTO-DETECTOR READOUT" PhotoDet 2012, LAL Orsay

*** fused quartz = quartz = fused silica = amorphous** SiO_2

Radiator geometry optimization with Geant4

We study more then 10 different geometries (show only 3 the most promising)

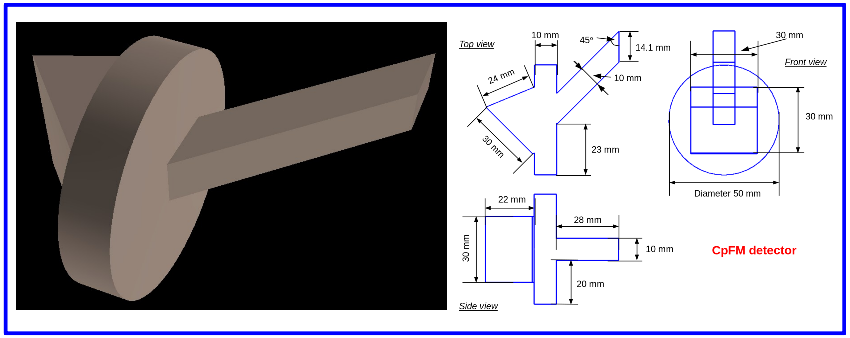

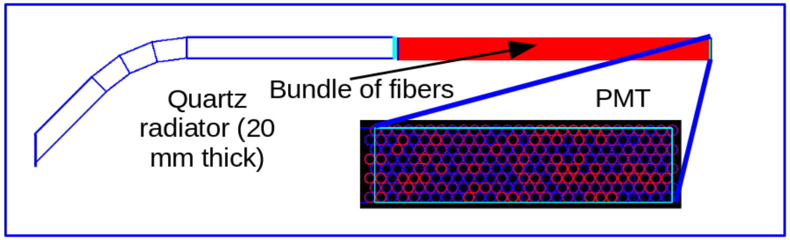

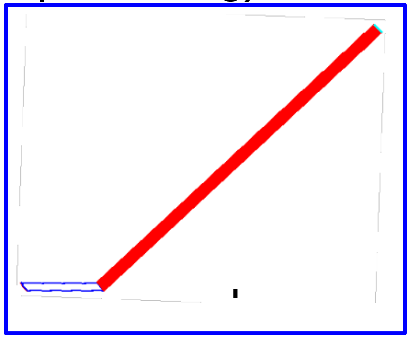

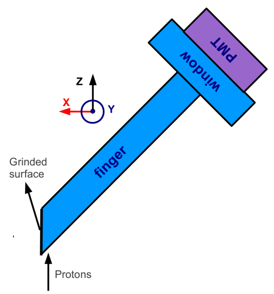

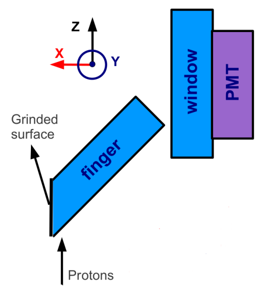

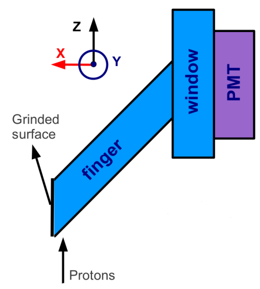

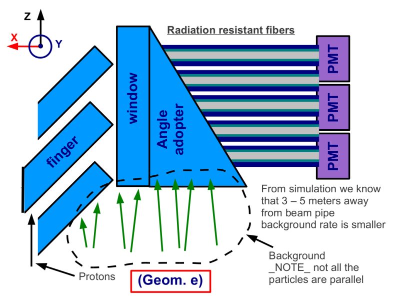

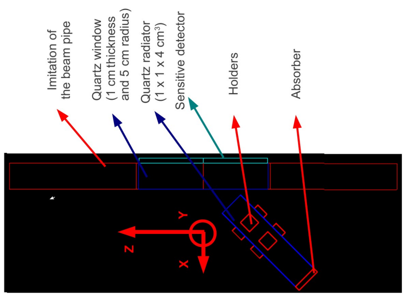

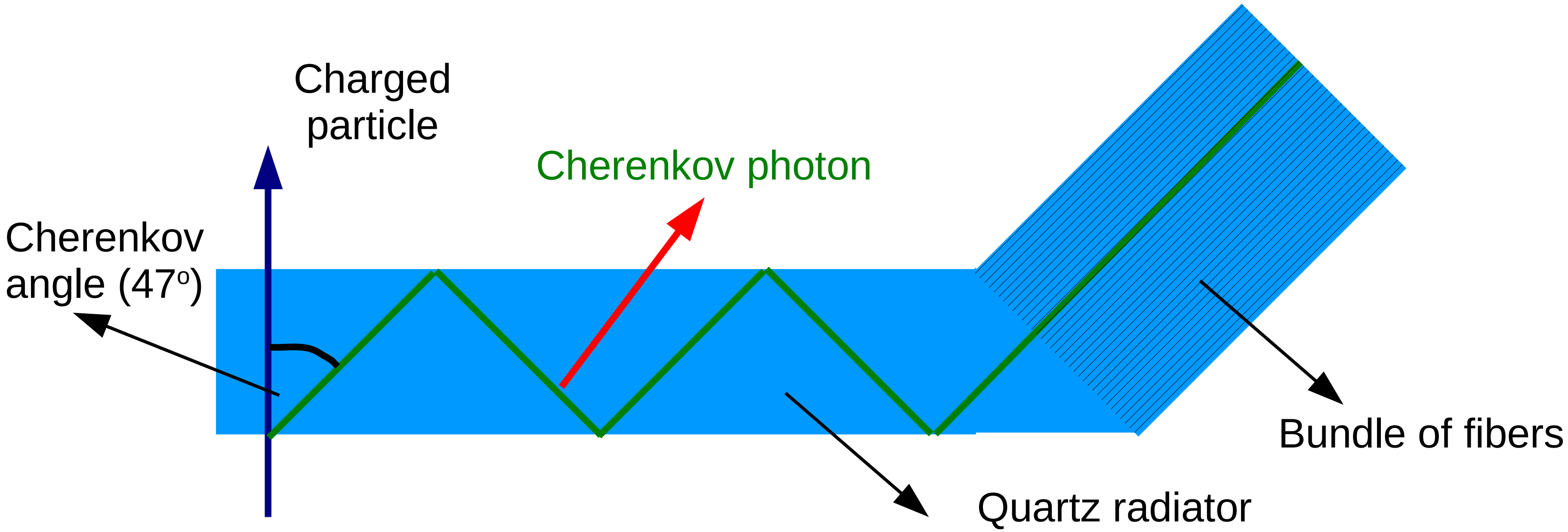

Test of the first CpFM prototypes with 500 MeV/c electrons (October 2013)

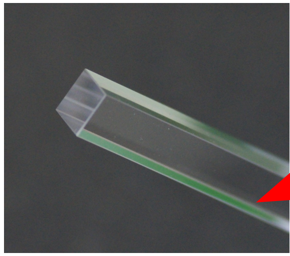

Quartz finger
100 x 10 x 10 mm^3

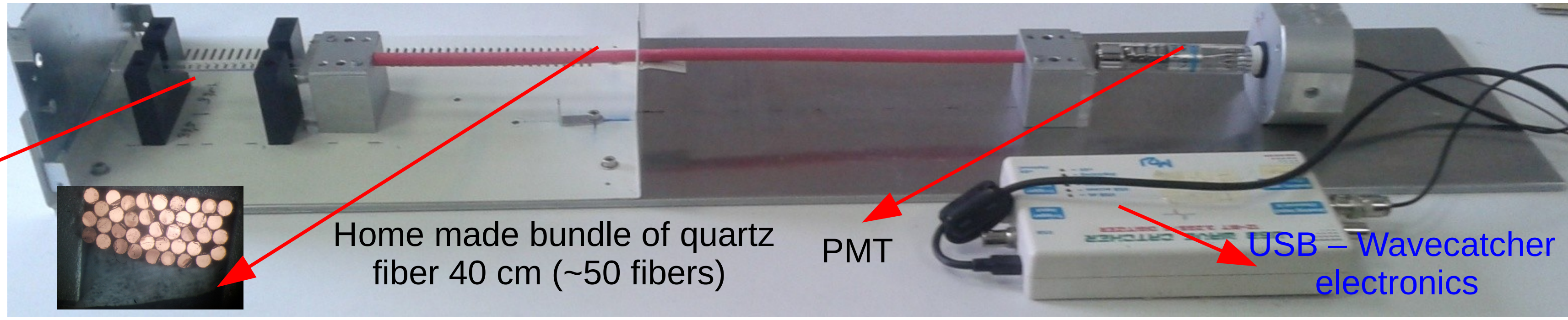

Main results

Direct coupling

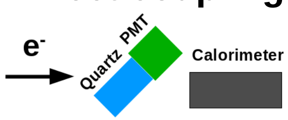

With Geant4 simulation we obtain (63) p.e. per electron

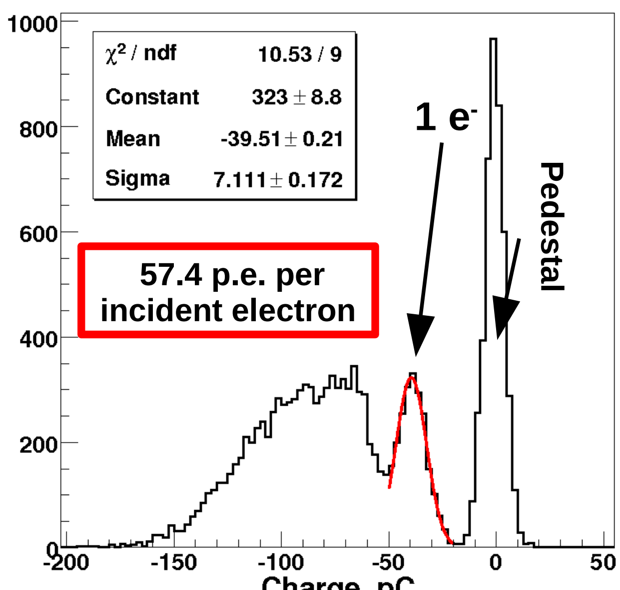

With bundle

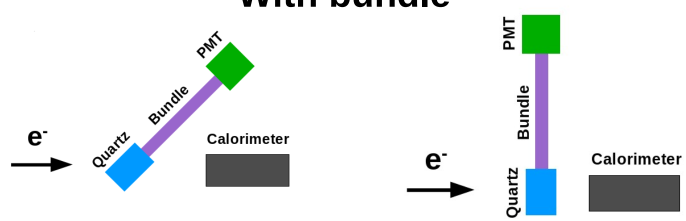

With Geant4 simulation we obtain 1 p.e. per electron

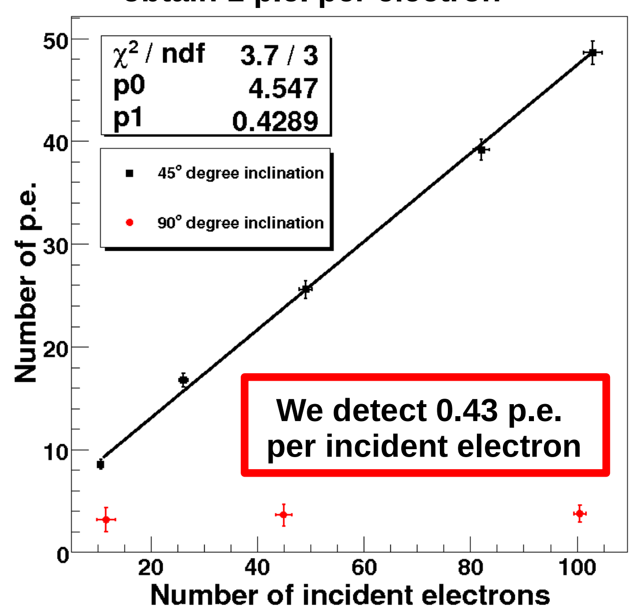

<u>Note:</u> p.e. Photo-electron (detected photon)

This successful test (validated by the simulation) encourage us construct full size of CpFM

See next slide

L. Burmistrov, et al. "Cherenkov detector for proton flux measurement for UA9 project." conference proceedings IEEE, 2013.

CpFM

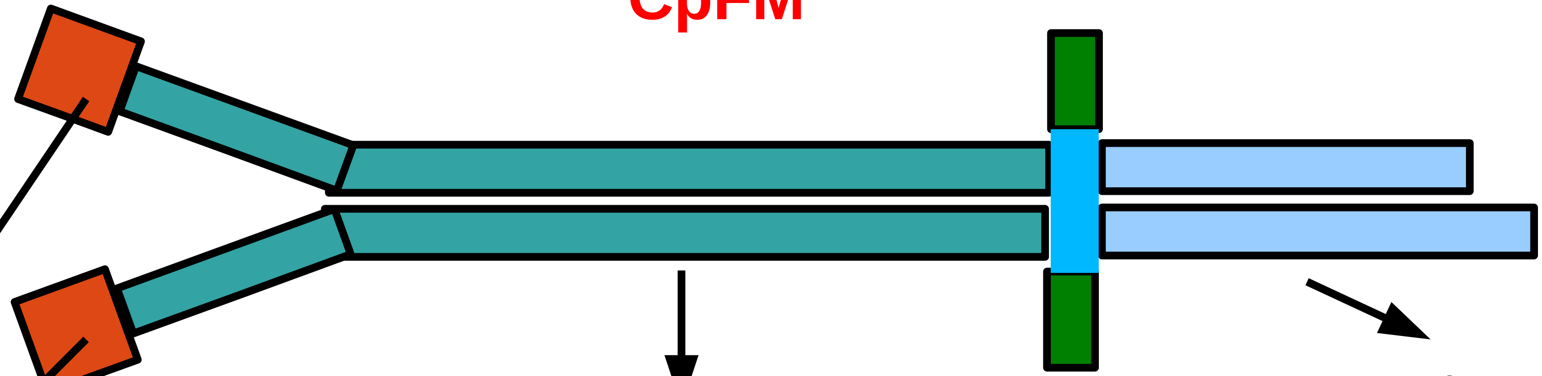

Light guide bundle (4 m) 200 fibers

Quartz (~ 30 cm) radiator and "flange"

HAMAMATSU PMT (R7378A) with radiation hard fused silica incoming window

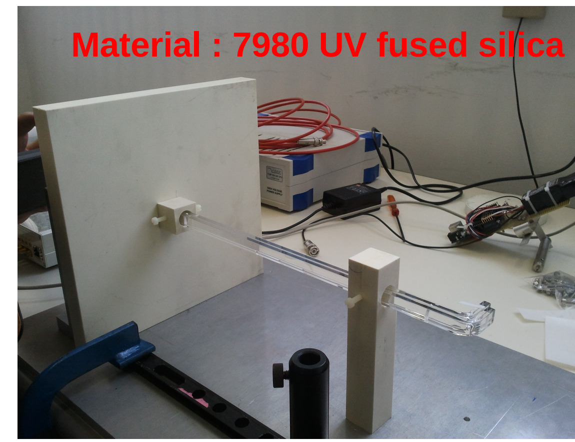

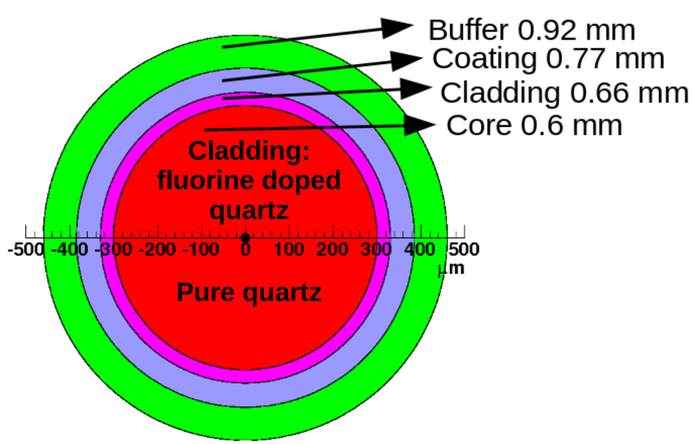

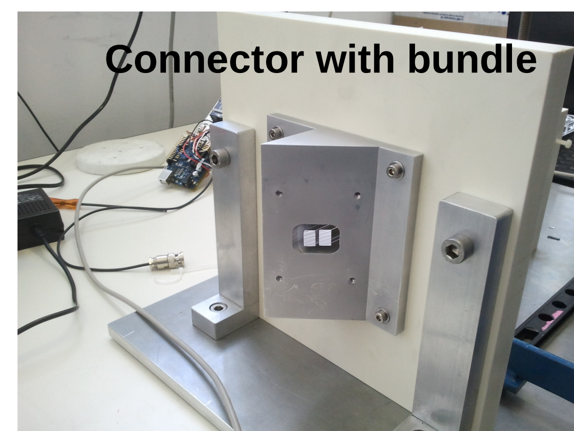

Test at BTF (April 2014)

Beam **T**est **F**acility (BTF) at Frascati

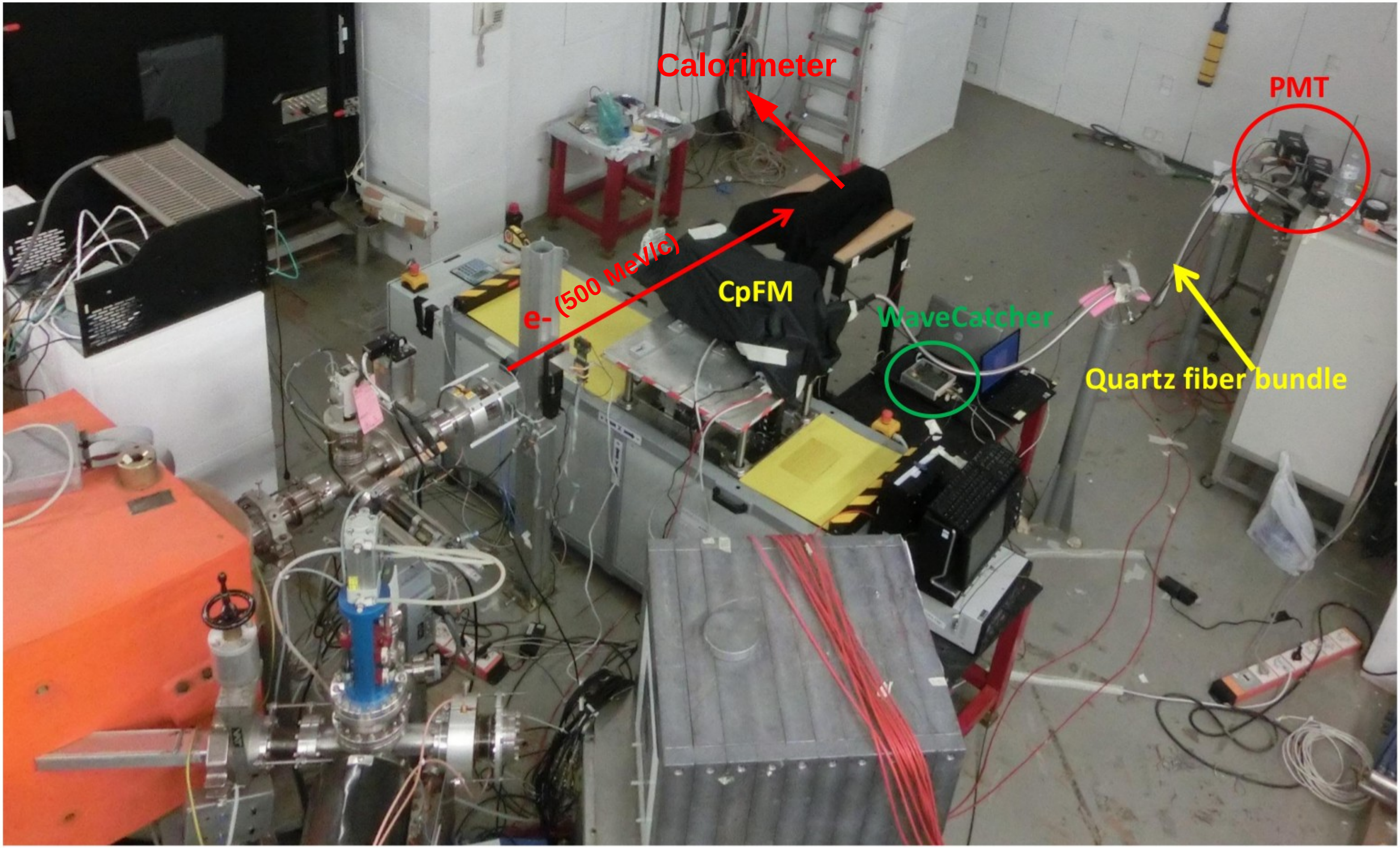

Results (1)

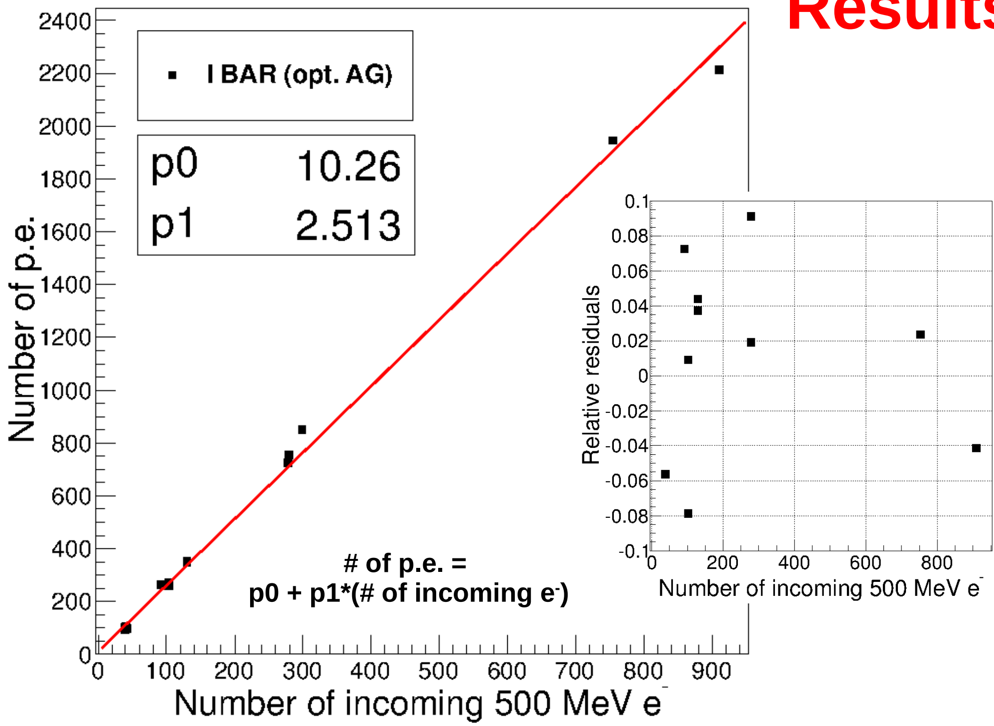

Configuration: Quartz + bundle + PMT

PMT gains :

H.V = 800 → PMT gain = 7.75×10^5

H.V = 900 → PMT gain = 1.84×10^6

H.V = 1000 → PMT gain = 4.00×10^6

H.V = 1100 → PMT gain = 8.07×10^6

→ Detector shows good linearity

Effect coming from the view port

Configuration: <u>Quartz + PMT</u> vs Configuration: <u>Quartz + glass 3.85 mm + PMT</u>

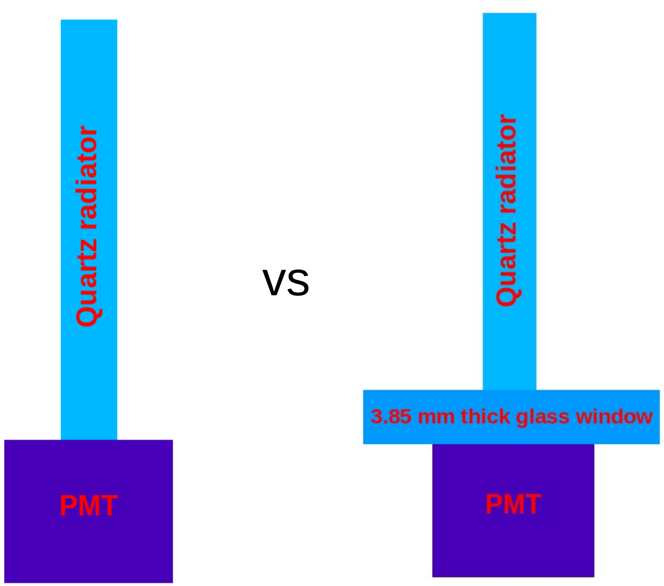

We observe factor of two signal degradation

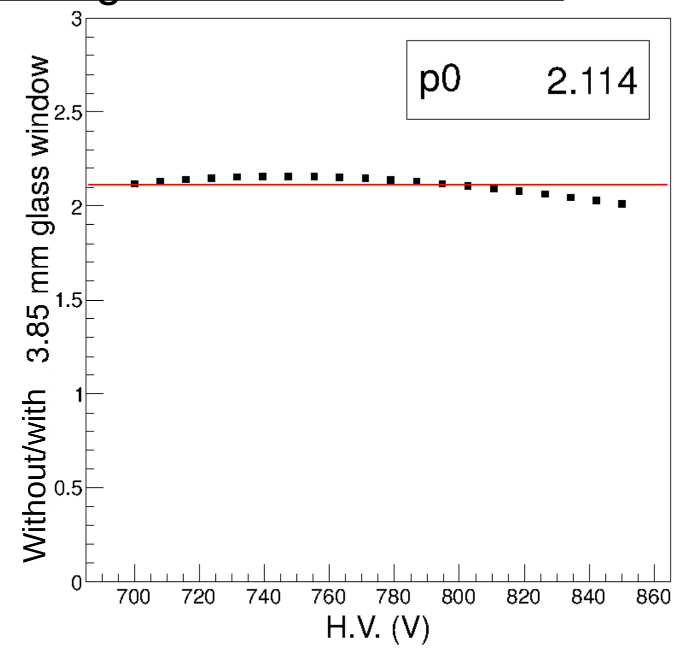

Results (2)

Quartz + 4 mm thick glass window (emulating view port) + bundle + PMT

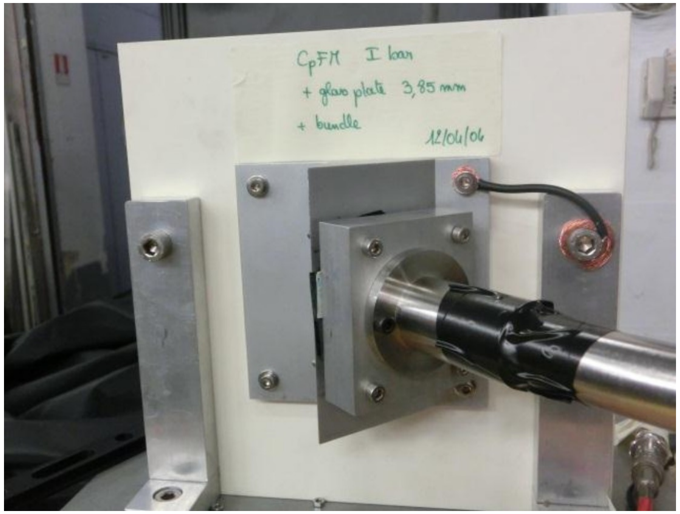

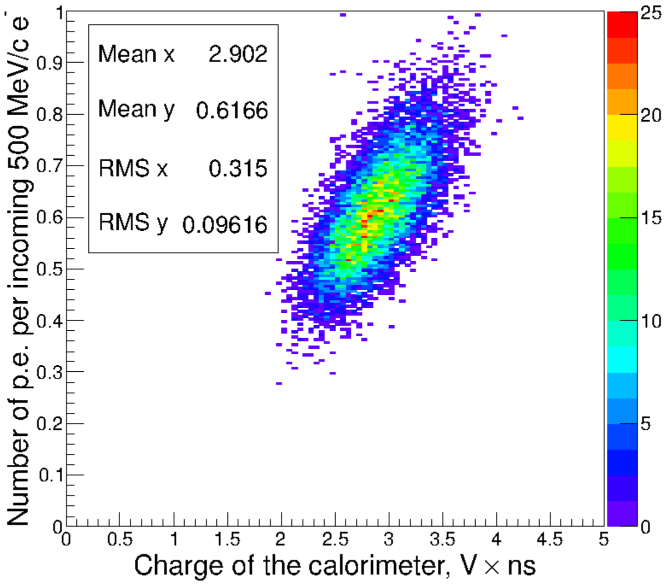

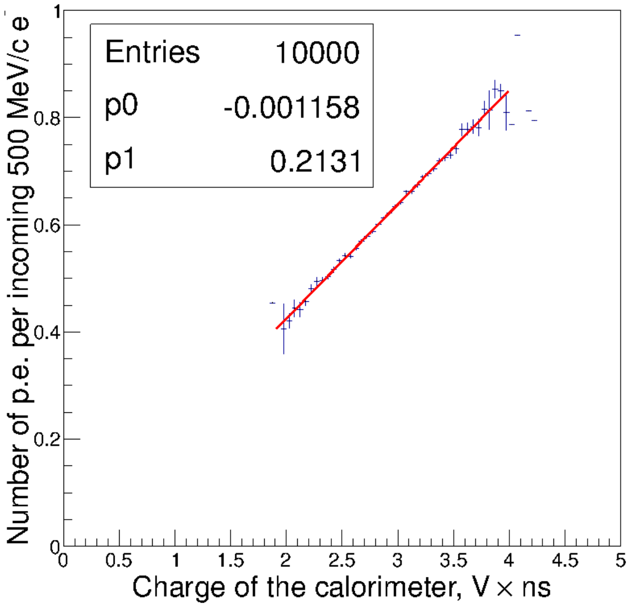

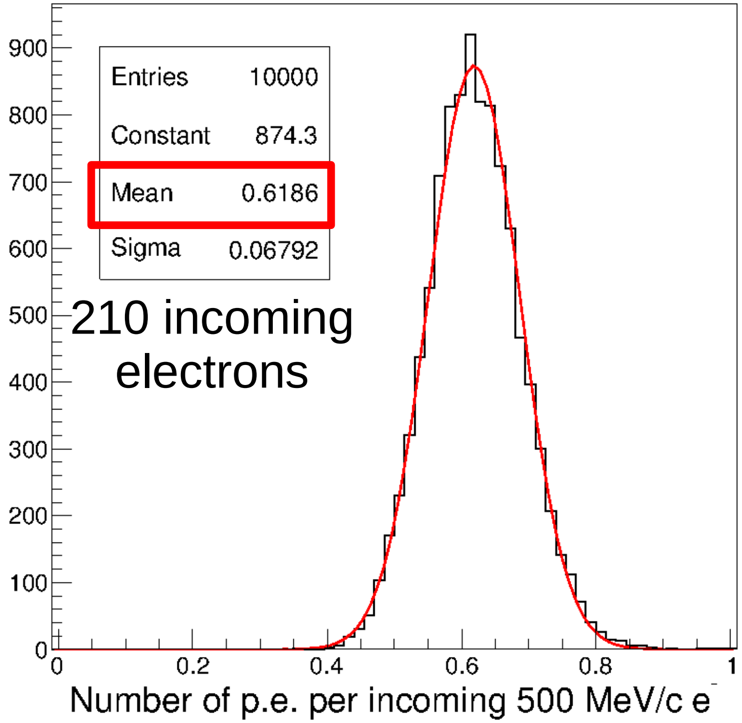

Using information from the calorimeter one can make correction on number of incoming electrons.

Applying this correction we obtain 15 % resolution for 100 incoming electrons.

We detect 0.62 p.e. per incoming electron

Possible improvement of the CpFM

We obtain 15 % resolution (for 100 incoming electrons) with present geometry of the CpFM

$$\frac{1}{0.62 \text{ p.e.} \times 100 \text{ particles}} = 13\%$$

I-shape

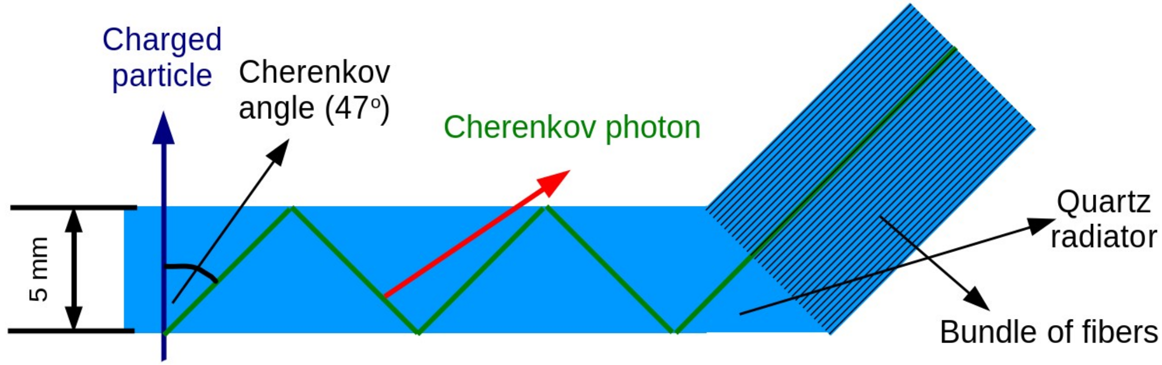

$$\frac{1}{0.62 \text{ p.e.} \times \mathbf{6} \times 100 \text{ particles}} = 5\%$$

↓

Increase amount of light
With L-shape geometry

L-shape

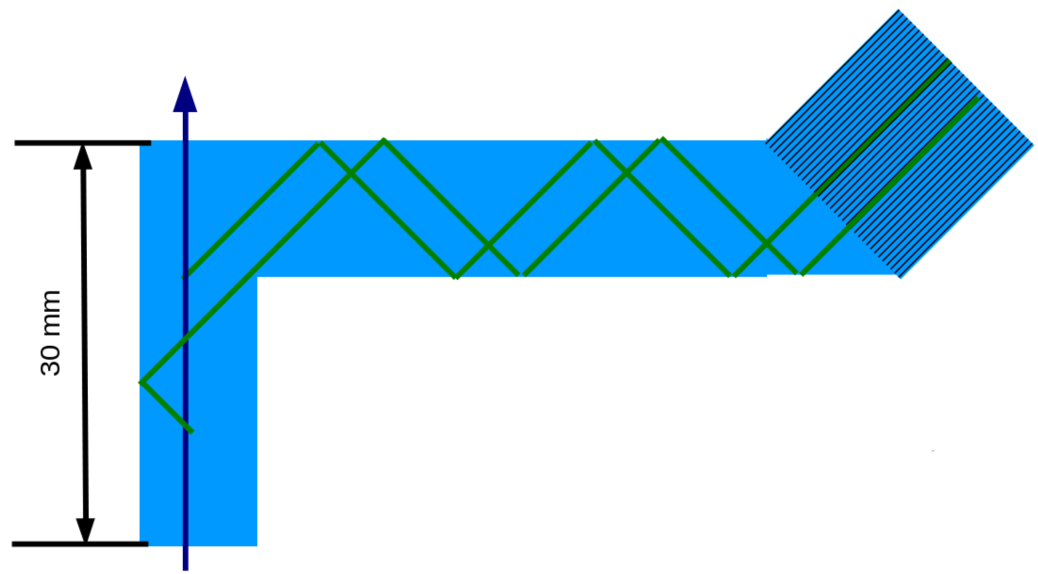

Conclusions

- Measured resolution for proton counting is going to be around 15 % (for 100 protons)

- We found that interface viewport between beam vacuum and tunnel is going to reduce the signal by factor of two.

- **The produced CpFM detector fulfills the needs for proton counting of the secondary beam.**

- We will make final calibration at H8 (CERN) test in October (2014)

- CpFM is going to be installed at SPS this winter.

Acknowledgements

The authors would like to acknowledge BTF team, especially Luca Foggetta, for their support during beam test.

We are grateful to Igor Kirillin for his useful discussion about crystal collimation.

Backup

Standard CERN cables (signal)

CpFM integration

Simone Montesano (CERN - EN/STI)

Cable	Diametre (mm)	Attenuation (dB / 100 m)				Price (CHF / m)	Notes
		10 MHz	100 MHz	200 MHz	800 MHz		
CB50	5	4.5	14.5	21	44	0.96	Standard SPS
CK50	15.30	0.67	2.5	3.7	8.2	5	“Low loss”
CC50	10.3	1.9	6.8	9.8	21	2.1	
CKB50	11.5	0.5	1.5	4.3	6.3	4	“High immunity” Not in storage Connectors?
LDF1-50	8.763	1.254	4.049	5.798	12.084		proposed by LAL

Charged particle interaction with crystal structure

Interaction of the charged particle with amorphous body is very different from interaction with crystal structure.

Amorphous

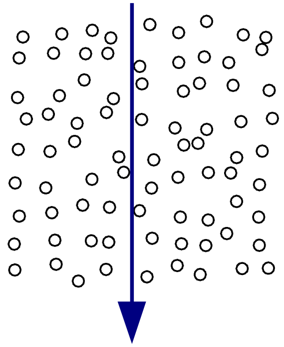

Crystal

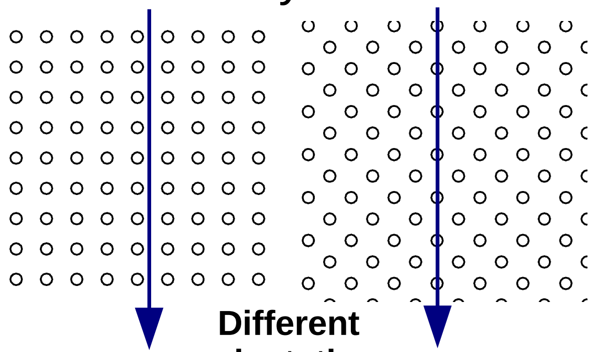

Robinson M. T. Computer studies of the slowing down of energetic atoms in crystals Phys. Rev. – 1963. – Vol. 132. – P. 2385–2398.

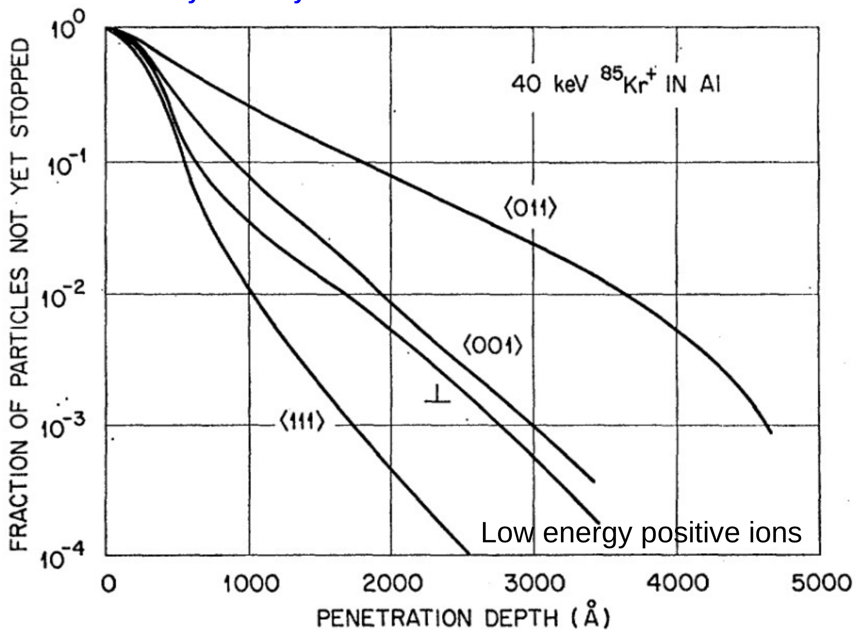

Fig. 17. Experimental data of Piercy, Davies, McCargo, and Brown (Ref. 11) for the penetration of 40-keV $^{85}Kr^{+}$ into an Al monocrystal. The curve marked ⊥ was obtained at normal incidence (9° from ⟨112⟩); the others were obtained with the beam 28° from the surface normal. The penetrations have been corrected for the angle of incidence.

Piercy G. R. Experimental evidence for the increase of heavy ion ranges by channeling in crystalline structure // Phys. Rev. Lett. – 1963. – Vol. 10. – P. 399–400.

In case of charged particle oriented along crystal lattice planar **channeling** effect occurs. The channeled particles have anomalously low energy losses in channeling mode.

Experimental observation with light ions (He^{3} with E ~ 30 MeV)

Erginsoy C. Anisotropic energy loss of light particles of MeV energies in thin silicon single crystals // Phys. Rev. Lett. – 1964. – Vol. 13. – P. 530–534.

BTF – (Beam Test Facility) at Frascati

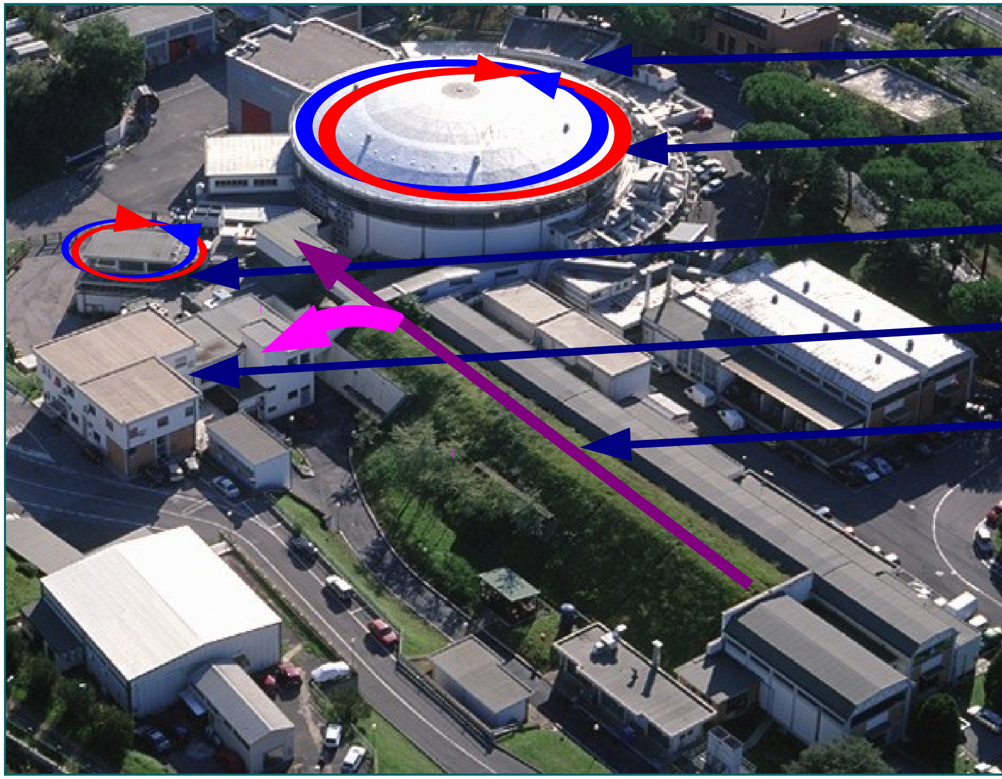

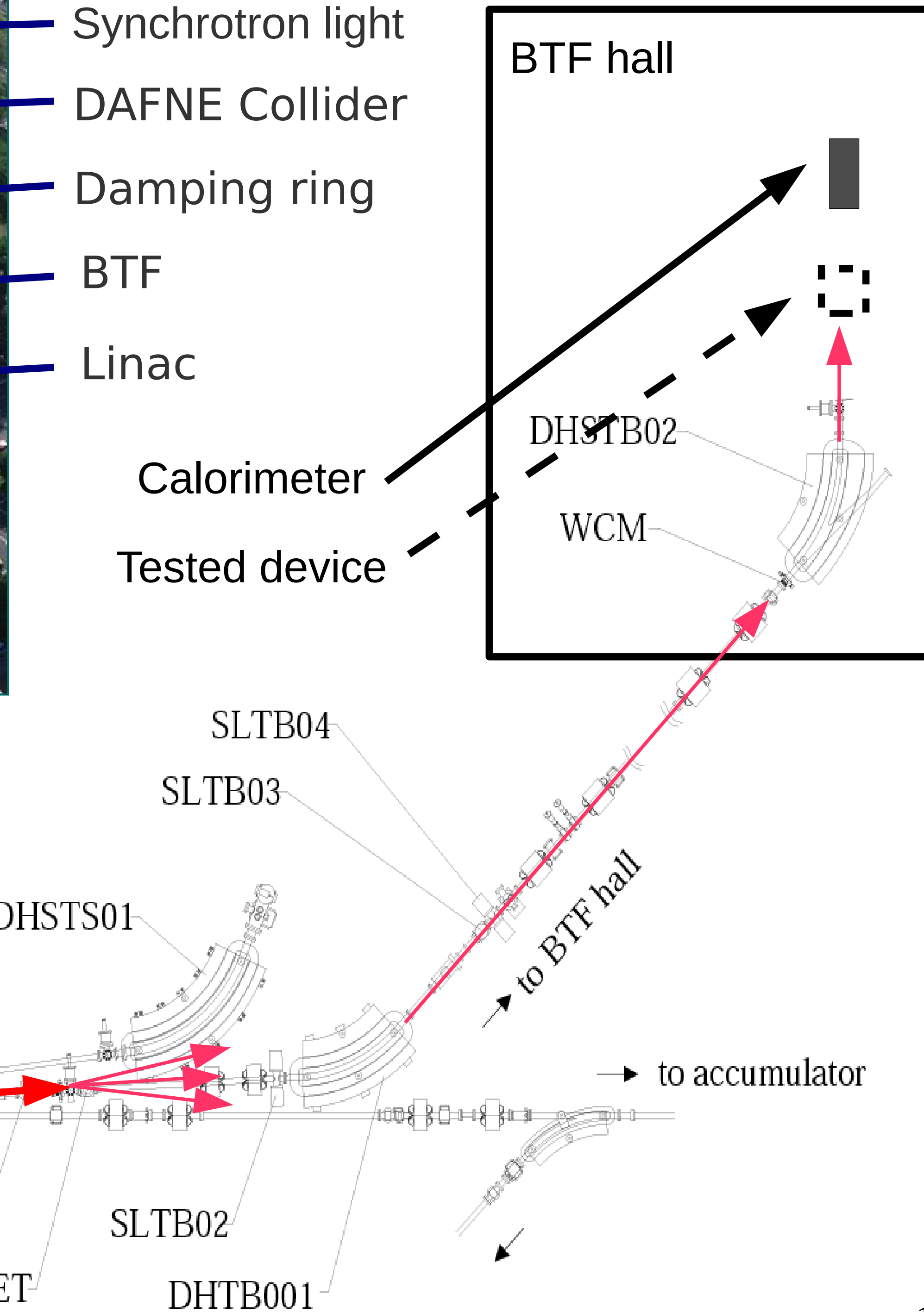

Characteristics of the e^- beam @ BTF

Particles number:	1 - 10^5 e^-/pulse
Energy:	25 – 500 MeV
Frequency:	20 Hz
Pulse duration:	10 ns

Radiation hardness of the CpFM components

Annuel Radiation levels close to the pipe: γ dose = 10 Mrad

thermal neutrons fluence = 10^{14} n/cm²

protons fluence = 10^{13} p/cm²

(1 Gy = 100 rad)

Quartz radiation hardness

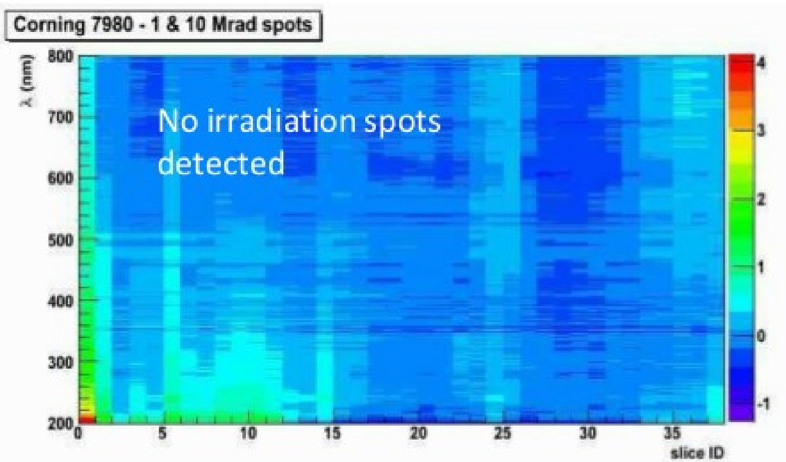

M. Hoek, RICH 2007

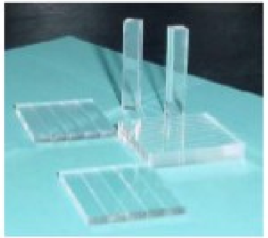

3 fused silica types (Corning 7980, Schott Lithosil Q0, Heraeus Suprasil 1) irradiated with 150 MeV **proton** beam with dose levels: 100krad, 1Mrad and 10Mrad

→ **No significant radiation damage observed in any fused silica sample**

γ **Irradiation** (^{60}Co) with a dose of 11 MGy (1100 Mrad) : **stability of the samples** Heraeus Suprasil Standard & Infrasil, Spectrosil A and B (Saint-Gobain) and Corning 7940

➡ Our choice: Corning 7980 & Heraeus Suprasil

Effects of radiation on Photodetectors : PMTs

protons / neutrons /γ-rays

coloring of the glass

glass scintillation

- ➢deterioration of the borosilicate window transmittance but not for a fused silica window
- ➢increase of the dark current
- ➢no important change of the gain and quantum efficiency

No variation of the transmittance of quartz window

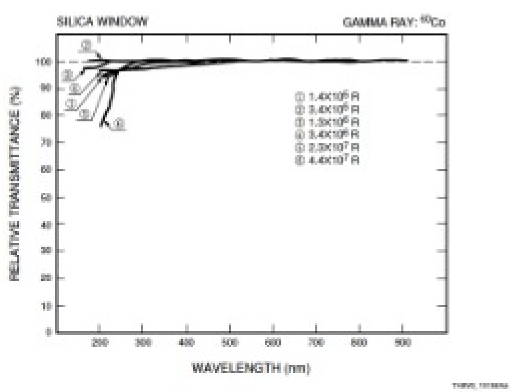

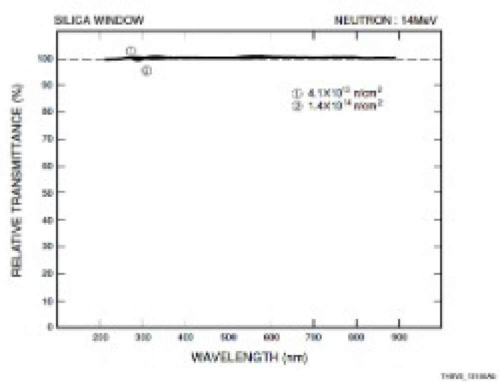

HAMAMATSU R762

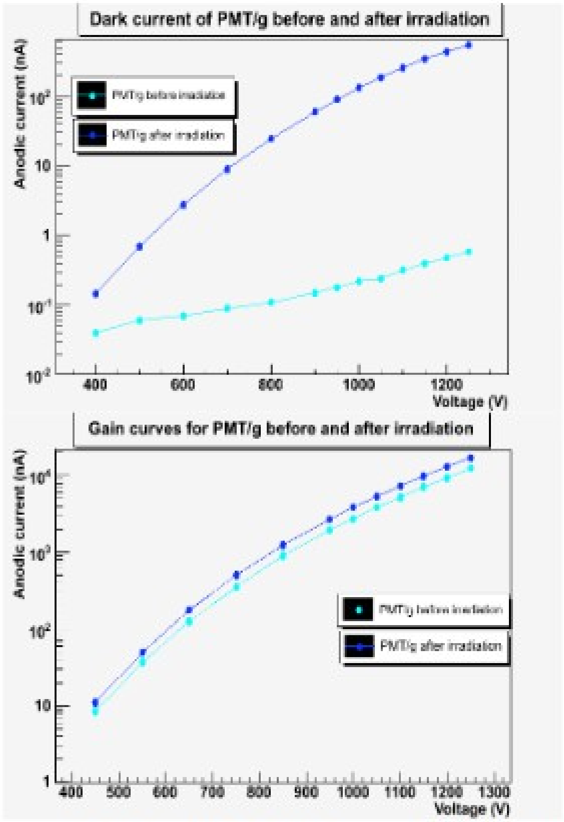

γ: 60Co, E = 1.22 MeV Dose = 20±1 Mrad

A. Sbrizzi LUCID in ATLAS

Our choices: Hamamatsu R762 & R7378A

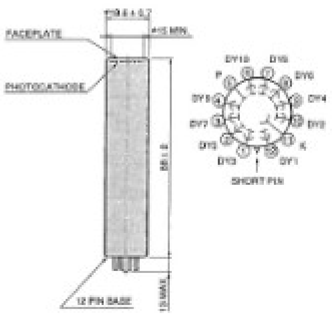

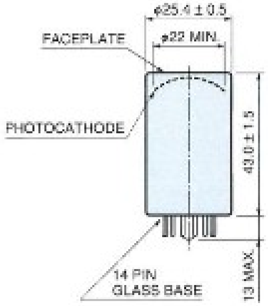

Véronique Puill (IPRD13)

Quartz + PMT

Charge measured by calorimeter

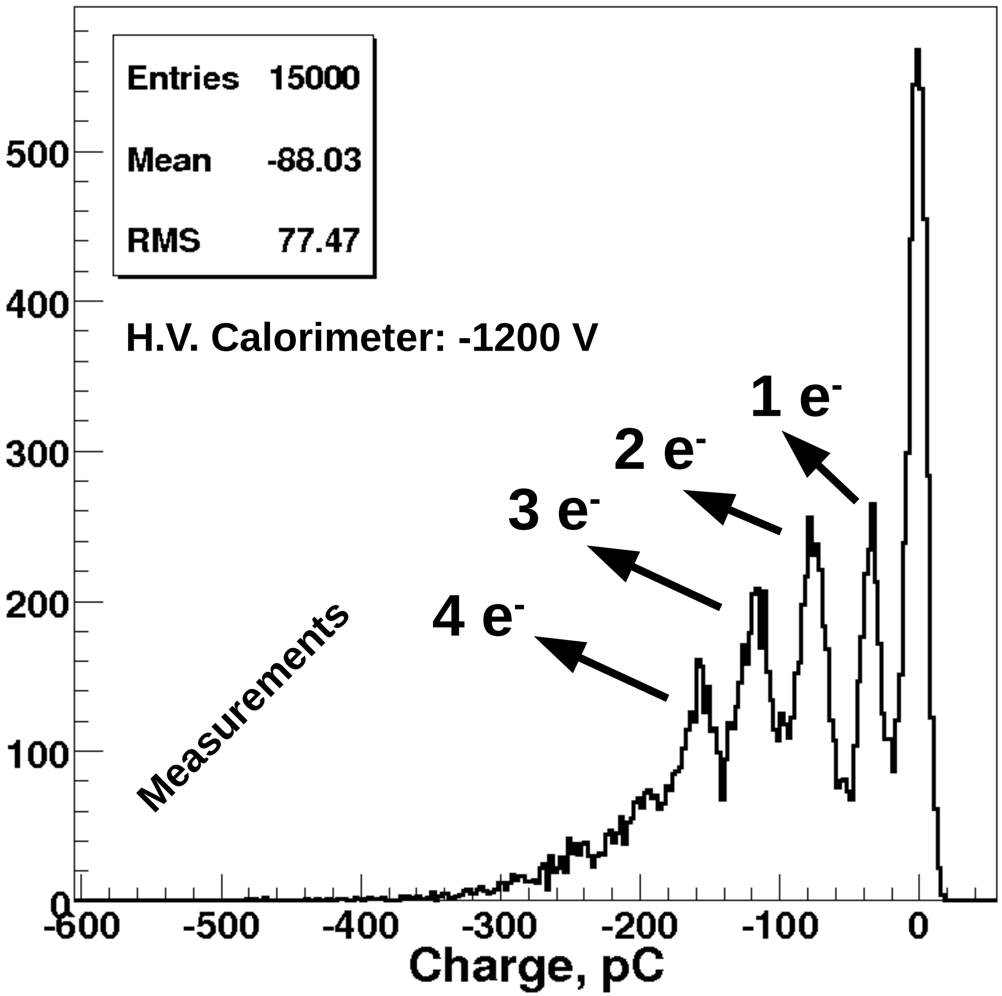

Charge measured by CpFM

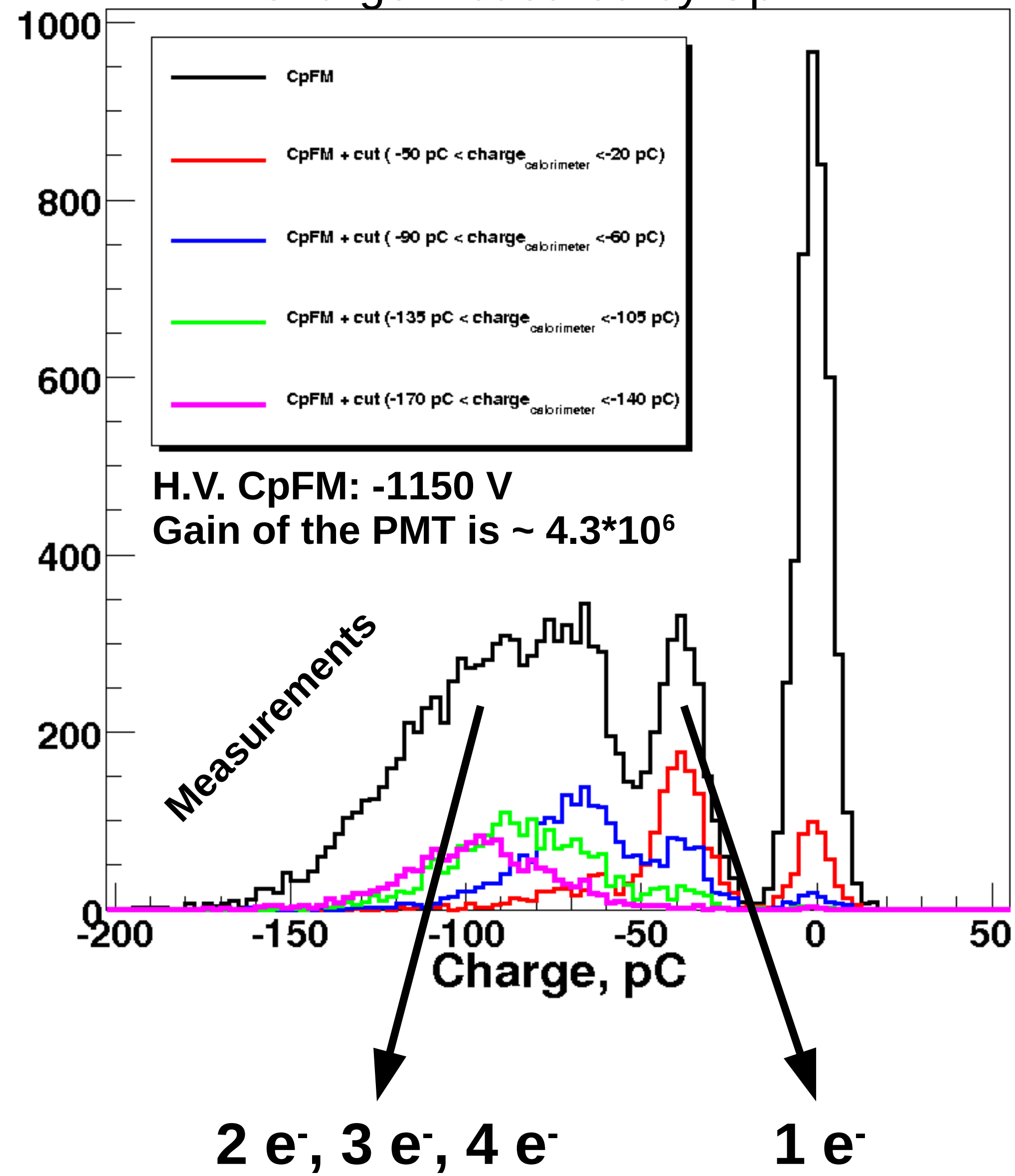

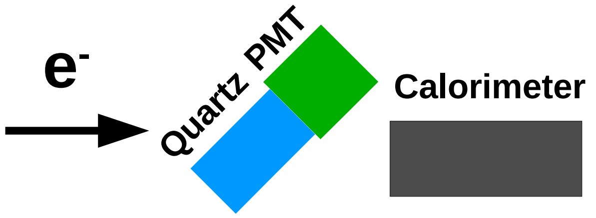

Saturation of the PMT ???

Optical fiber

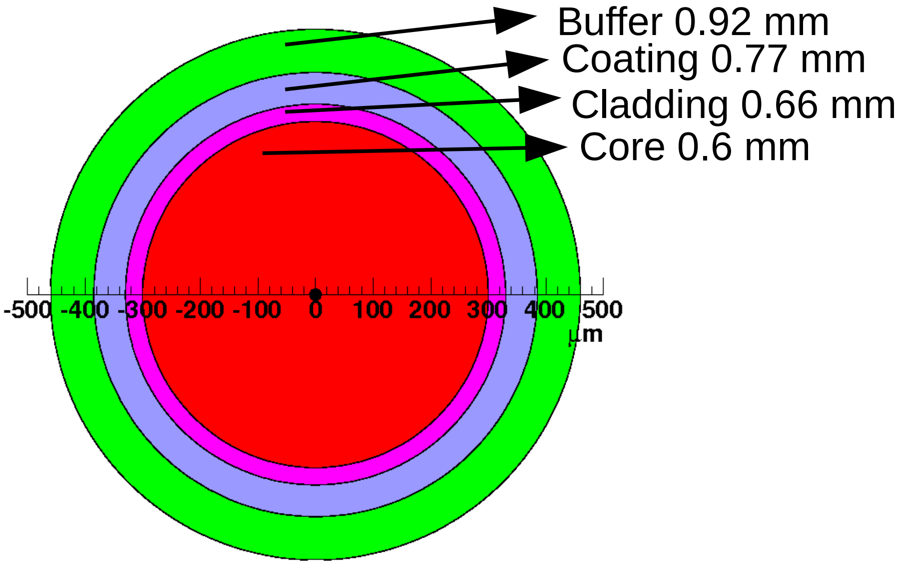

Numerical aperture => $0.22^2 = n_{Core}^2 - n_{Cladding}^2$

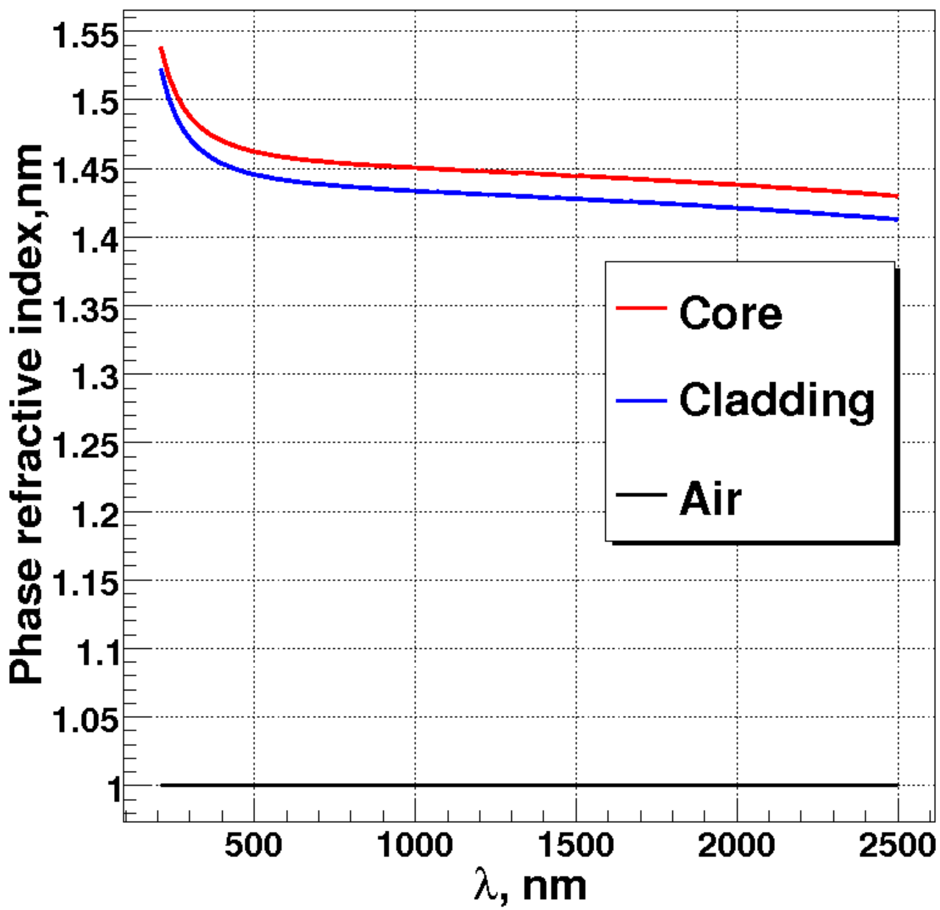

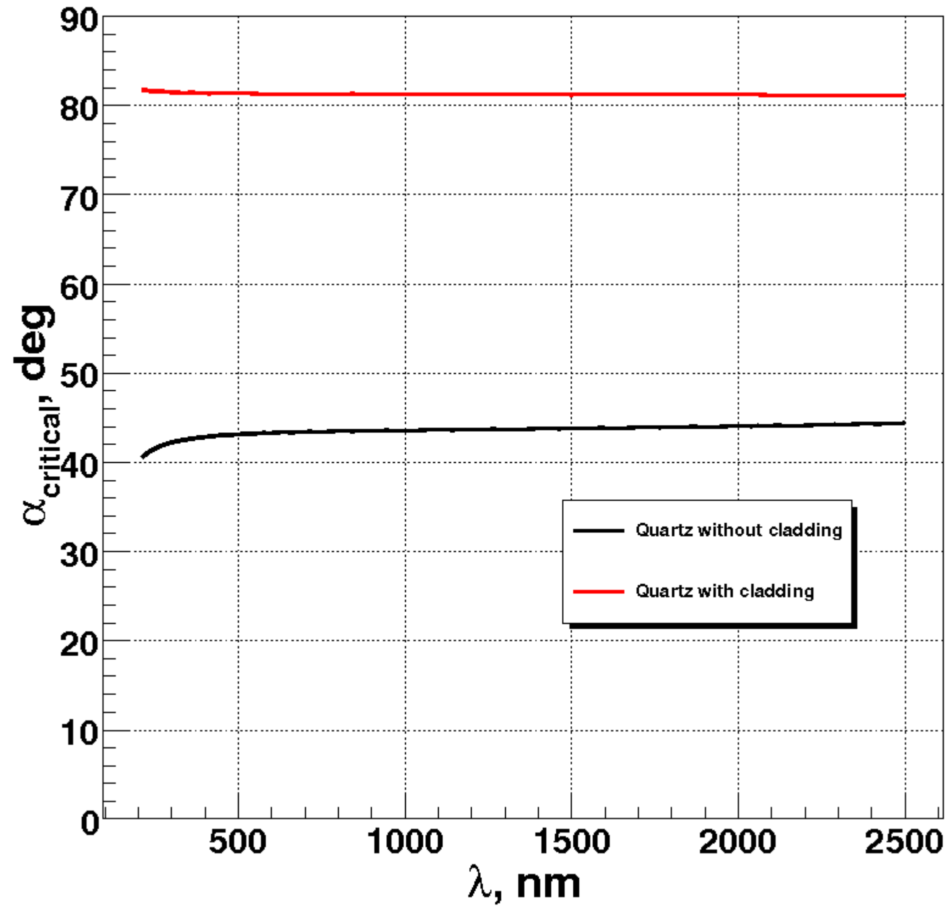

ZLUV - STANDARD TEFZEL JACKET SILICA/SILICA FIBERS		
CORE/CLADDING RATIO 1.07	CORE/CLADDING RATIO 1.1	CORE/CLADDING RATIO 1.2
ZLUV200/214/300T//500	ZLUV100/110/210T//1000	ZLUV200/240/340T//500
ZLUV300/321/450T//700	ZLUV200/220/320T//500	ZLUV300/360/510T//770
ZLUV400/428/570T//800	ZLUV300/330/430T//700	ZLUV400/480/630T//950
ZLUV600/642/760T//950	ZLUV400/440/550T//750	ZLUV600/7200/870T//1300
ZLUV1000/1070/1220T//1700	ZLUV400/440/550T//850	ZLUV800/960/1110T//1650
	ZLUV500/550/700T//900	ZLUV1000/1200/1350T//1700
	ZLUV600/660/800T//1000	ZLUV1000/1200/1350T//2020
	ZLUV800/880/1000T//1200	
	ZLUV909/1000/1100T//1300	
	ZLUV1000/1100/1250T//1500	
	ZLUV1000/1100/1300T//1600	

OTHER FIBER DIMENSION AVAILABLE ON REQUEST.
PLEASE CONTACT US FOR DISCUSSIONS.

NOTES:

1. HERAEUS FLUOSIL® SSU PREFORM.
2. EXCELLENT TRANSMISSION IN THE RANGE 180-1200 NM.
3. HIGH POWER LASER TRANSMISSION.
4. STRESS PROOF LOAD 100KPSI.
5. OPERATION TEMPERATURE FROM -40°C TO +150°C

VIEW A

FIBER CONSTRUCTION

EXAMPLE: ZUV600/660/770BT//920

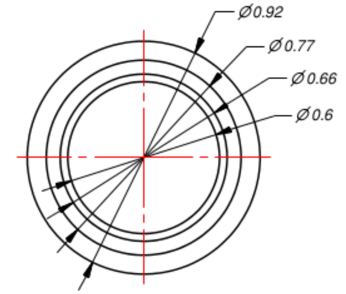

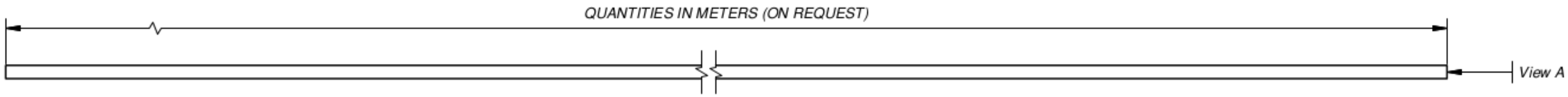

FIBER CODE EXPLANATION

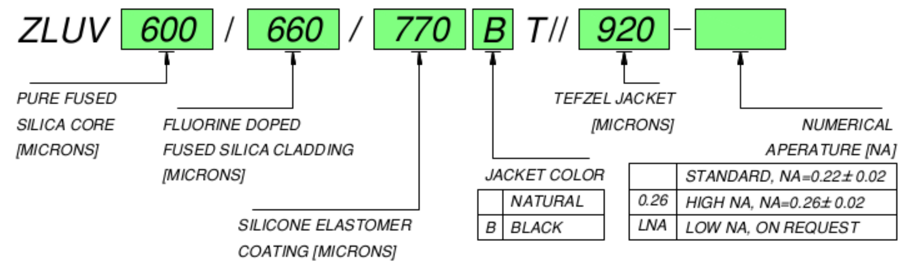

OTHER FIBER DIMENSION AVAILABLE ON REQUEST.
PLEASE CONTACT US FOR DISCUSSIONS.

TYPICAL FIBER ATTENUATION

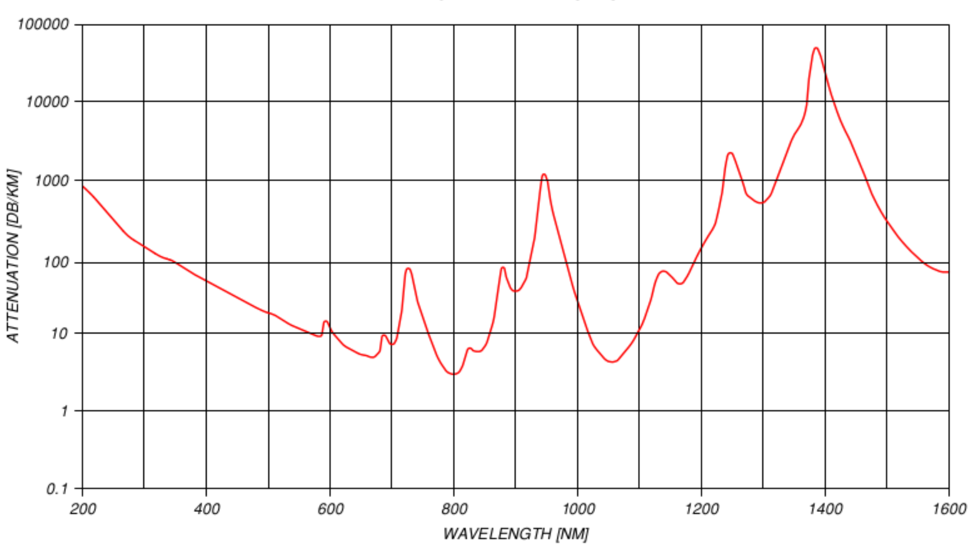

TITLE: ZLUV - TEFZEL JACKET SILICA/SILICA FIBERS			
SIZE: A3	DRAWING NO.: ZLUV-003-00		REV.: A
FILE NAME: ZLUV-TEFZEL.idw		ITEM NO.:	
		CODE NO.:	
		ORDER NO.:	
SCALE: DO NOT SCALE	DIMENSIONS ARE IN MM	SHEET 1 OF 1	

Number of p.e. as a function proton angle

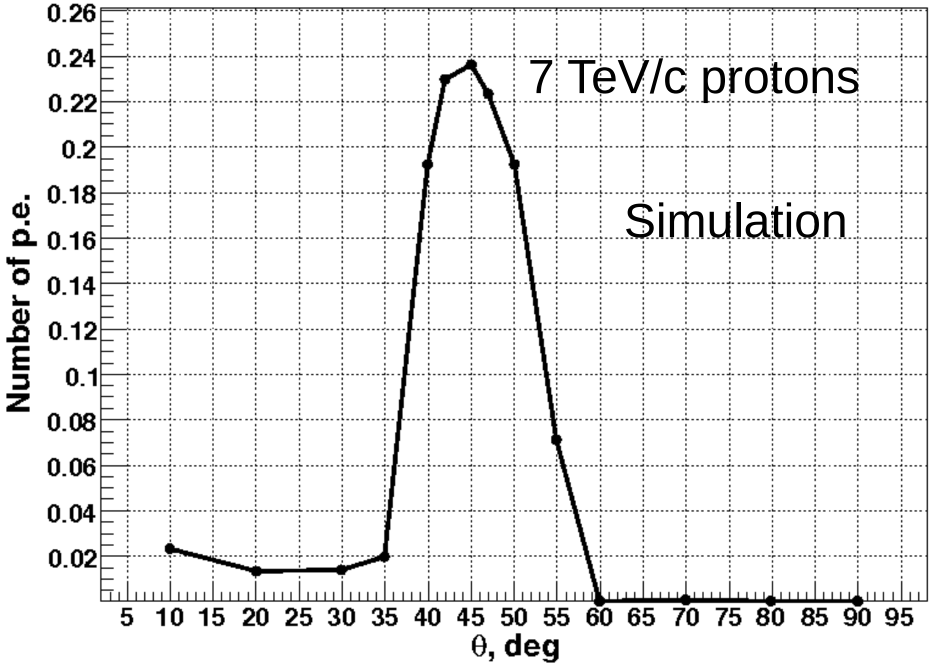

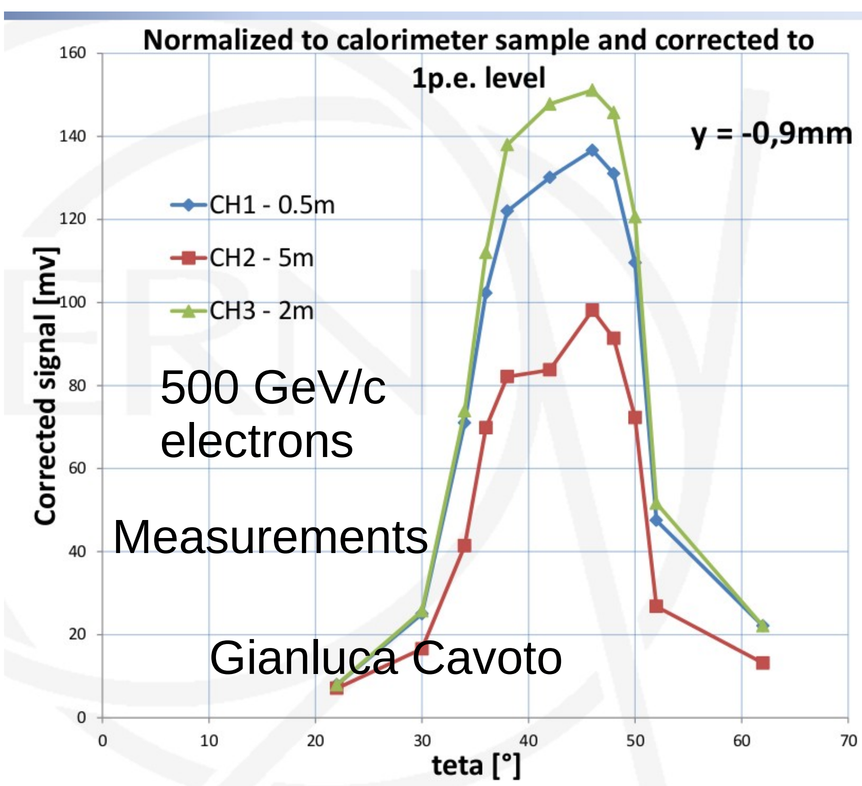

Photon detection efficiency (PDE) = 10 %

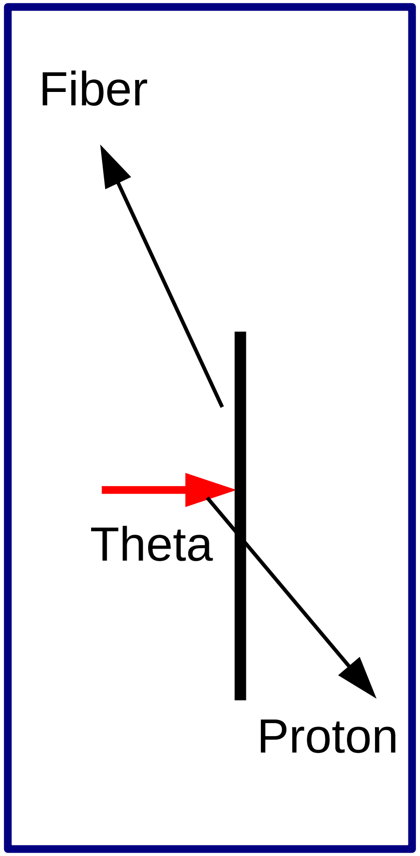

Geant4 simulation of the detector

Optical physics: Cherenkov effect and Snell's laws

$$\cos\theta_c = \frac{1}{n\beta}$$

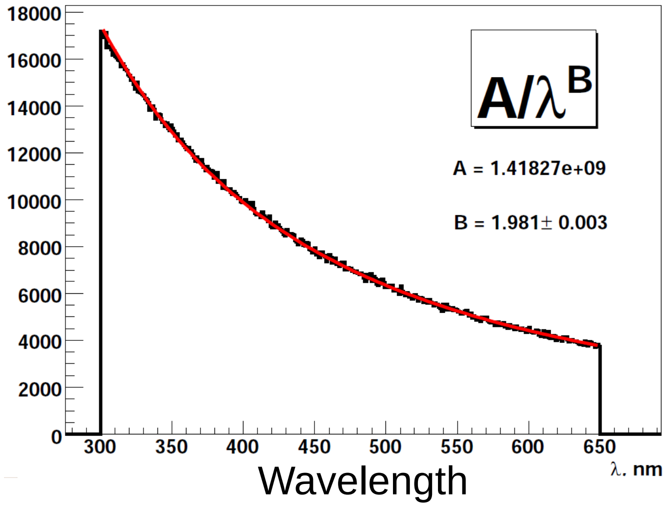

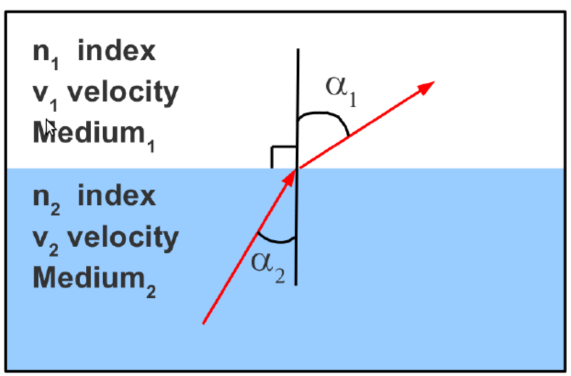

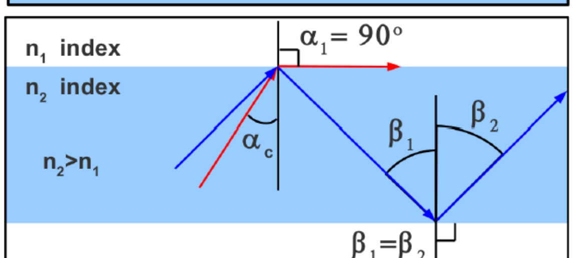

Optical properties of the quartz radiator:

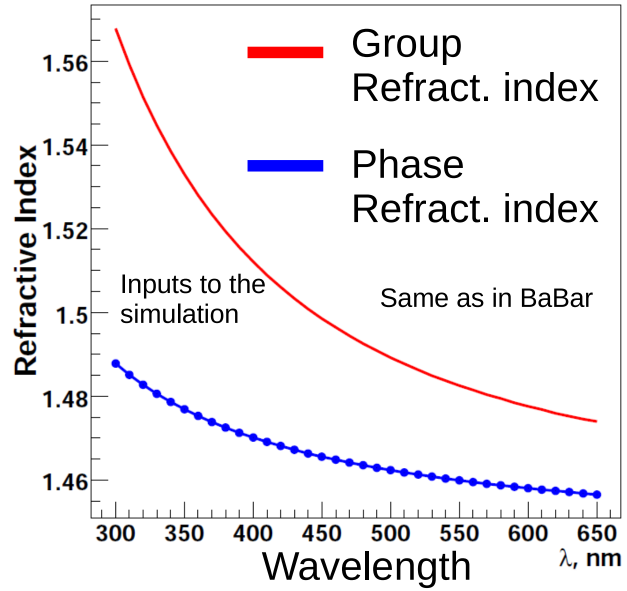

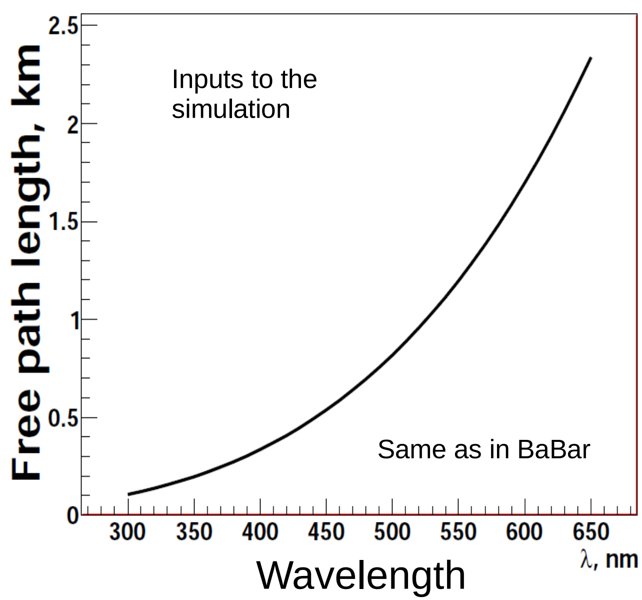

Properties of the quartz and mirror surfaces:

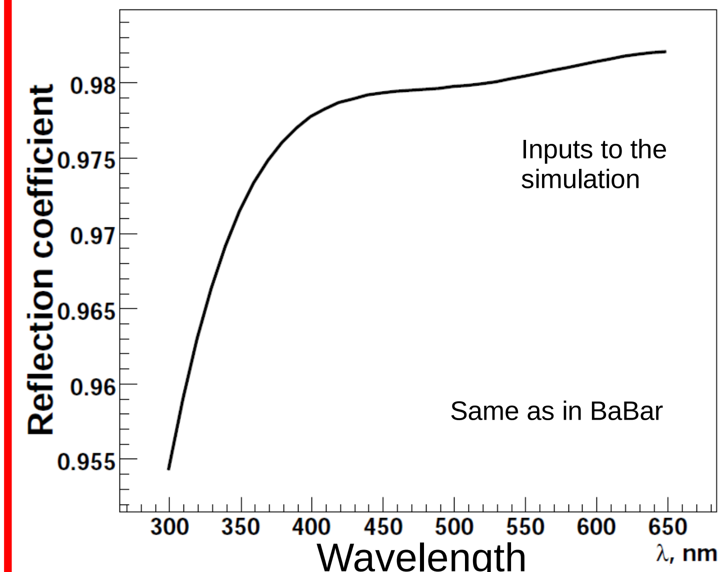

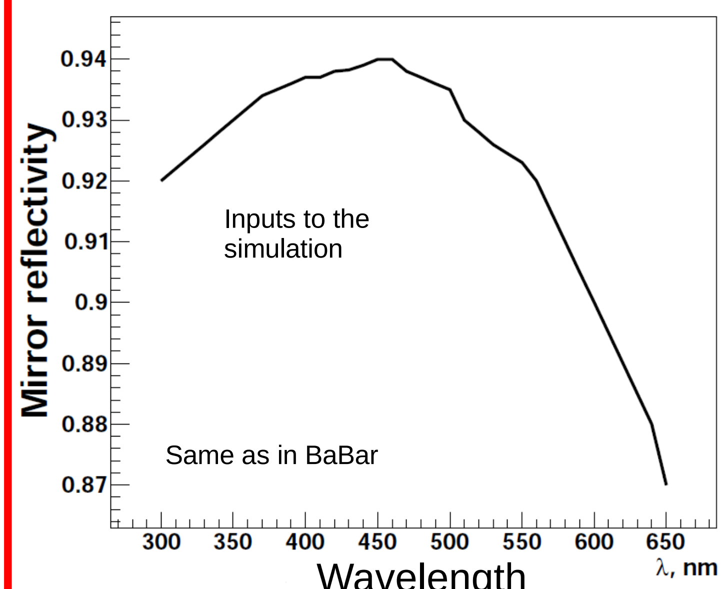

Loss rate reduction in the crystal area

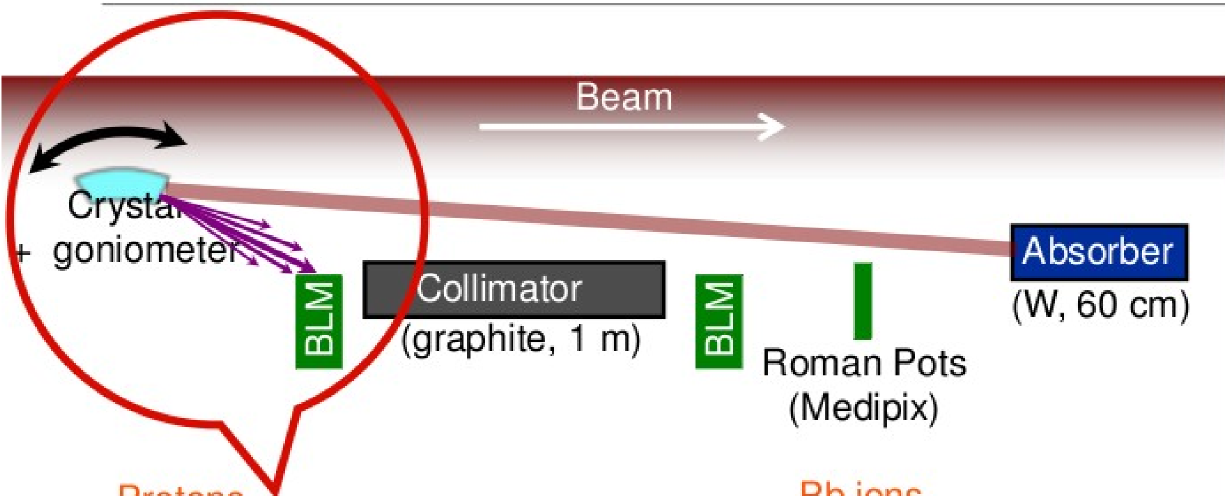

- Large loss reduction factor from "amorphous" to "channeling" orientation
  - 5÷20x reduction for protons
    3÷7x reduction for Pb ions
  - Best performance using a 1 mm long crystal
- Small discrepancy data/simulation
  - Mis-cut crystal modeled in simulation

Protons
Crystal aperture: 9 σ
Absorber aperture: 13.5 σ

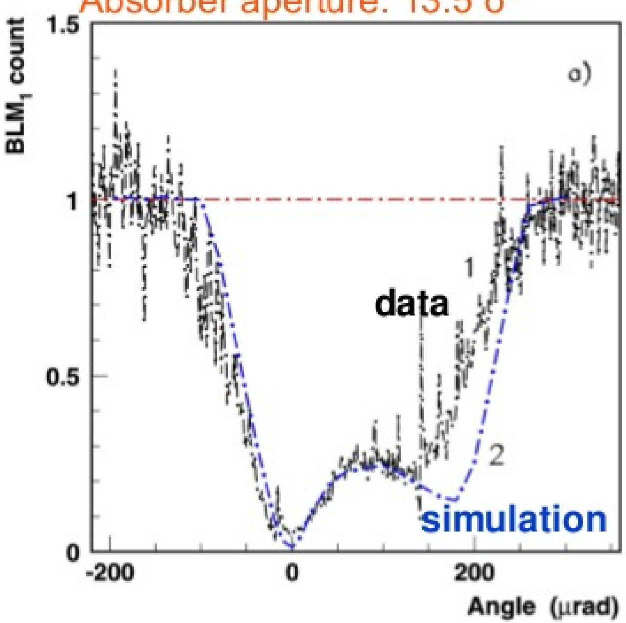

Pb ions
Crystal aperture: 3.5 σ
Absorber aperture: 7 σ

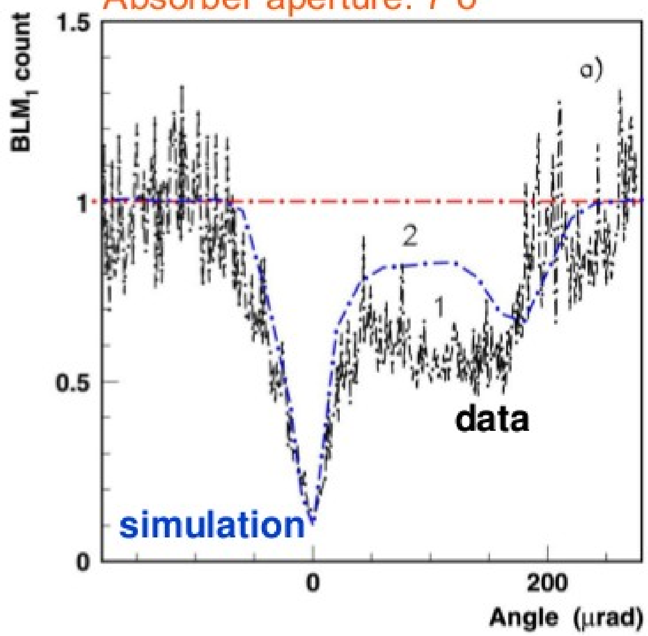

Perfect crystal   Crystal with mis-cut

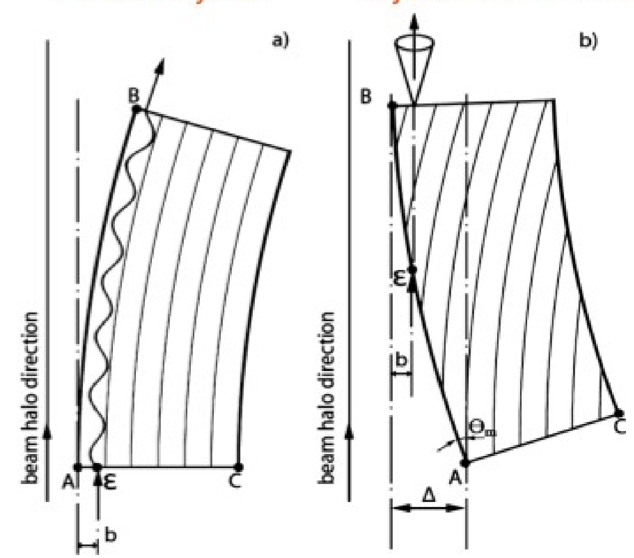

9

Walter Scandale

Apparatus to study crystal channeling and volume reflection phenomena at the SPS H8 beamline

(W. Scandale Rev. Sci. Instrum. 79, 023303 (2008); doi: 10.1063/1.2832638)

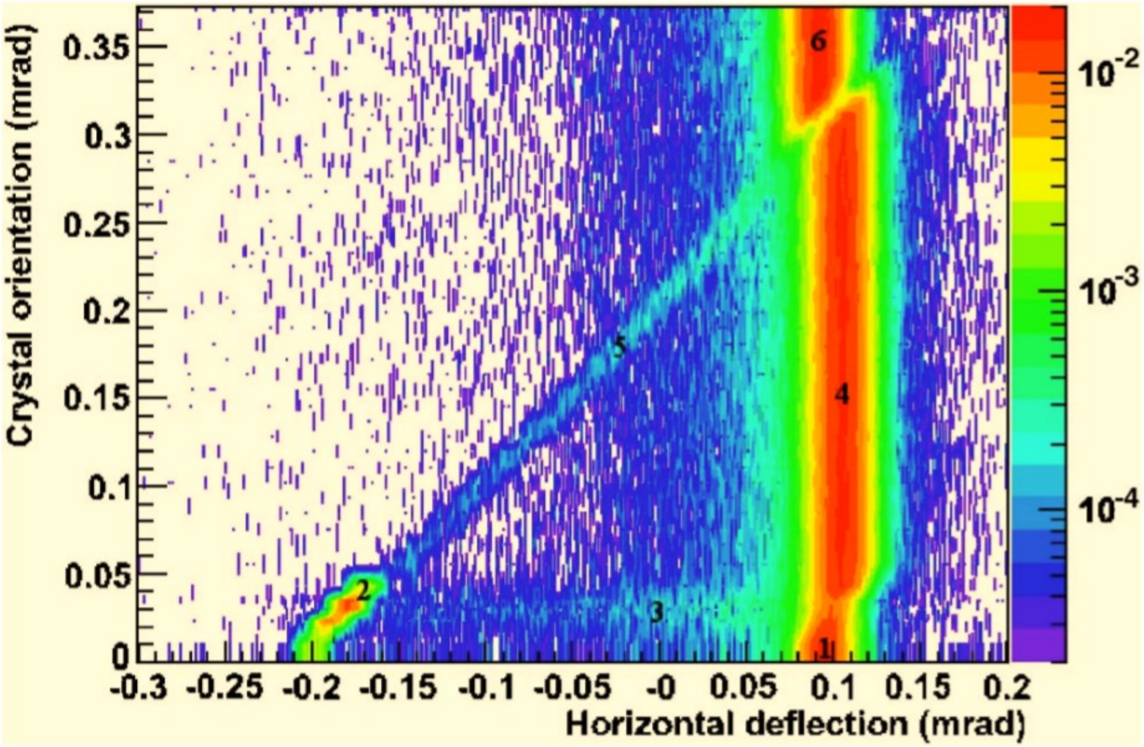

Region 1 pertains the beam traversing the crystal in a nonaligned orientation: no deflection is observed.

Region 2 The channeling peak is separated from the unperturbed beam by 278.2 mrad, which corresponds to the crystal bending angle measured with optical technique.

Region 3 A small fraction of the initially channeled particles
exits the channel due to an increase of the transverse energy dechanneled particles.

Region 4 The volume reflection extends over a wide angular area along the vertical axis: almost the whole beam is displaced by 10.4 +/- 0.5 mrad

Region 5 The particle may lose a fraction of its transverse energy and be trapped in the potential well

Region 6 volume reflection is no longer possible and the crystal is traversed by the incoming particles in a nonoriented condition, similar to region 1.

Principle of Beam Collimation

Walter Scandale

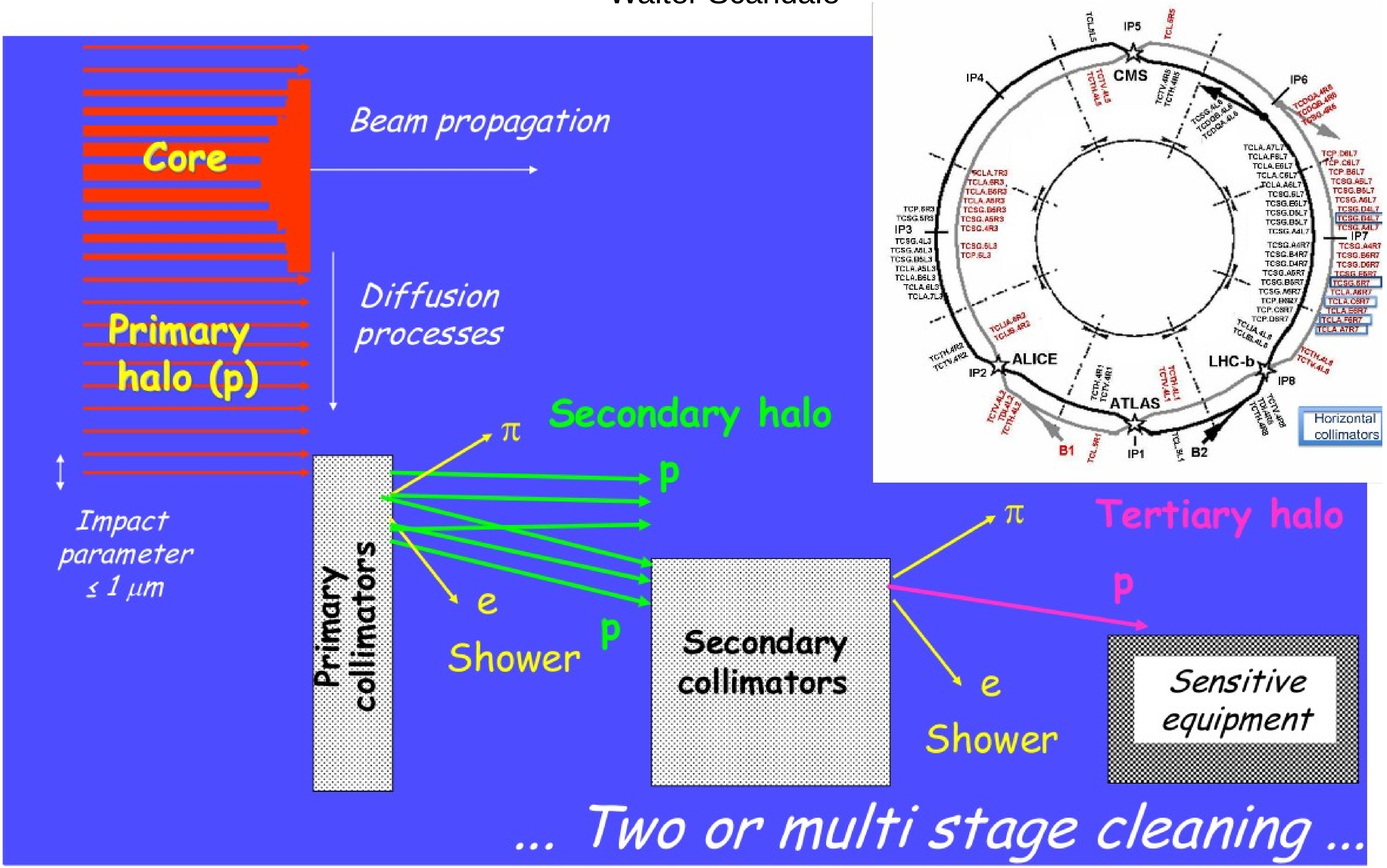

Collimating with small gaps

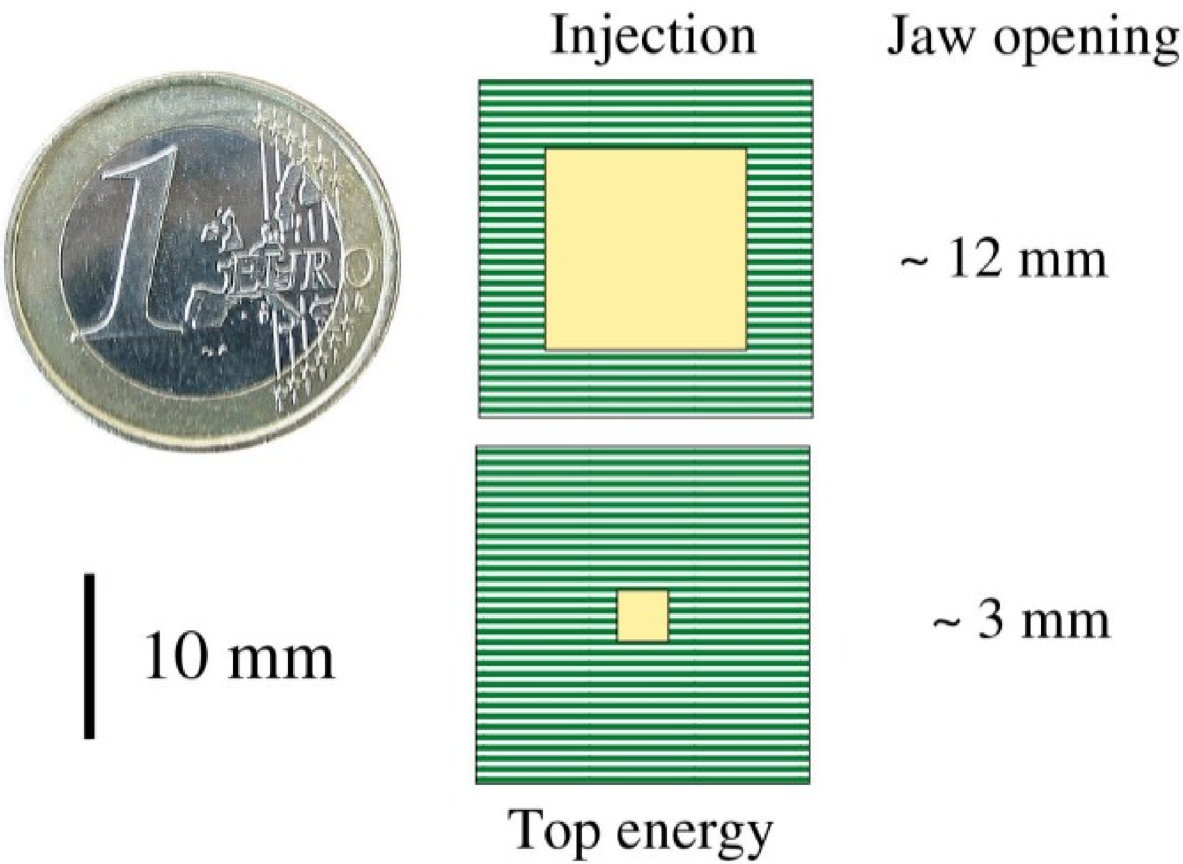

LHC beam will be physically quite close to collimator material and collimators are long (up to 1.2 m)!

- ***Precision positioning***
- ***Risk of damage to collimators!***
- ***Beam electro-magnetic fields interact with the collimator material!***

Machine impedance increases while closing collimators.
LHC will operate at the ***impedance limit*** *with collimators closed!*

Walter Scandale

Secondary curvature in bent crystal

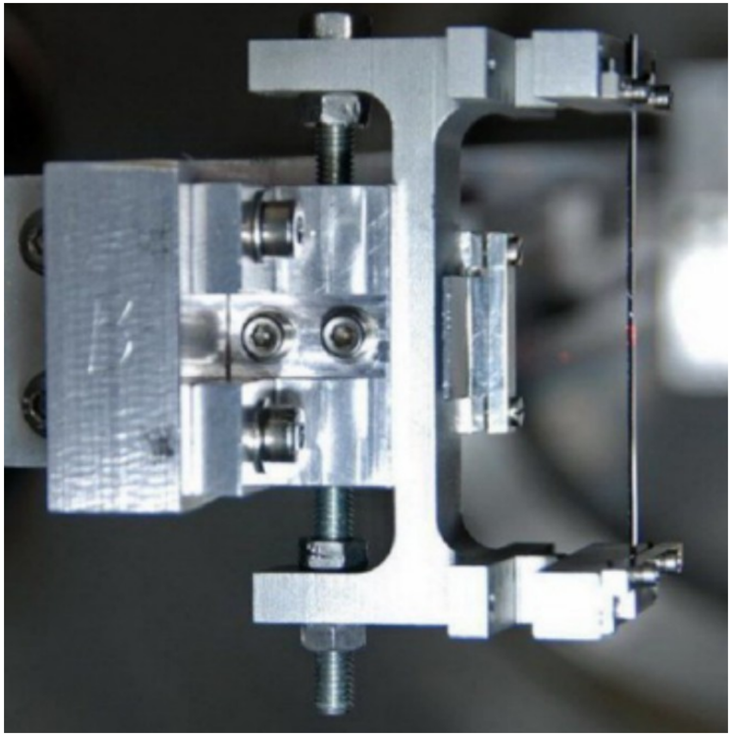

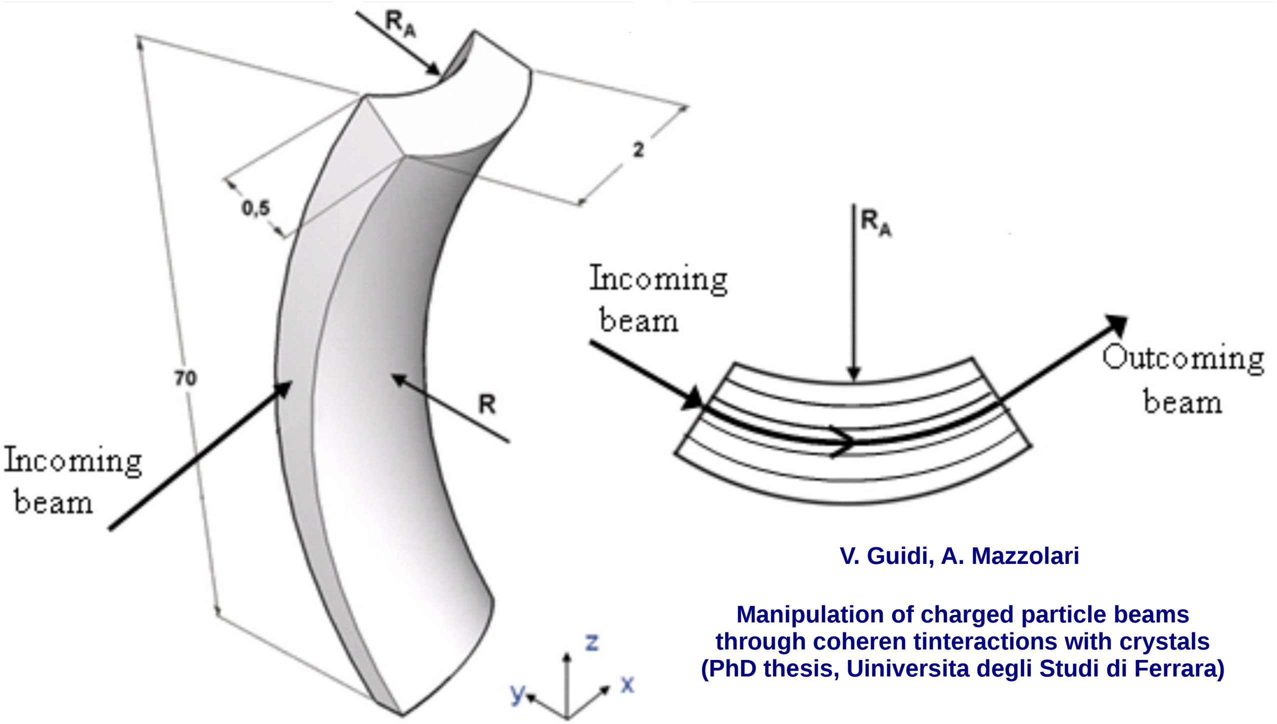

V. Guidi, A. Mazzolari

Manipulation of charged particle beams through coheren tinteractions with crystals (PhD thesis, Uiniversita degli Studi di Ferrara)

- Mechanically bent crystal
- Use of a secondary curvature of the crystal to guide the particles gives possibility to:
  - To curvature thin crystals
  - Secondary curvature is less parabolic (unlike primary ones)

Y. M. Ivanov, et al., "Observation of the Elastic Quasi-Mosaicity Effect in Bent Silicon Single Crystals" JETP Lett. 81, 99 (2005)

V. Guidi et al., "Tailoring of silicon crystals for relativistic-particle channeling " Nucl. Instrum. Methods Phys. Res., Sect. B 234, 40 (2005). (Anticlastic deformation)

Radiator geometry optimization with Geant4

We study more then 10 different geometries (show only 3 the most promising)

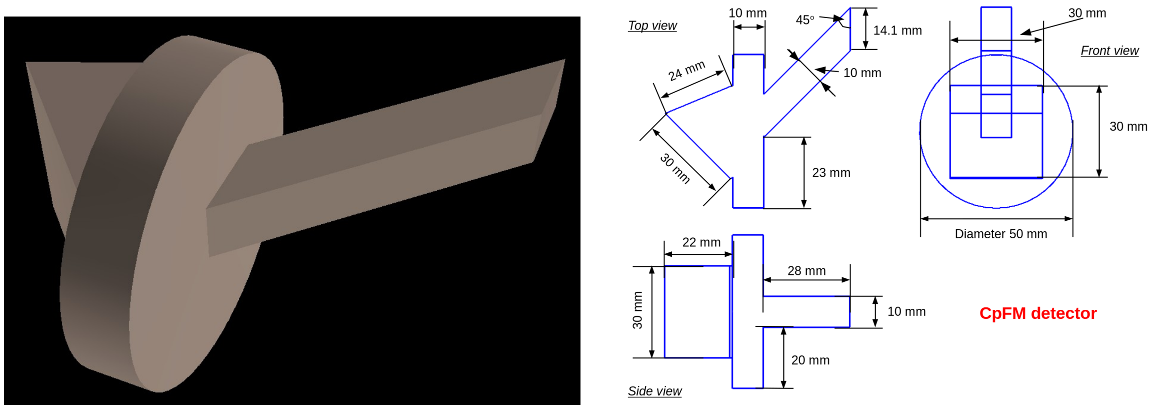

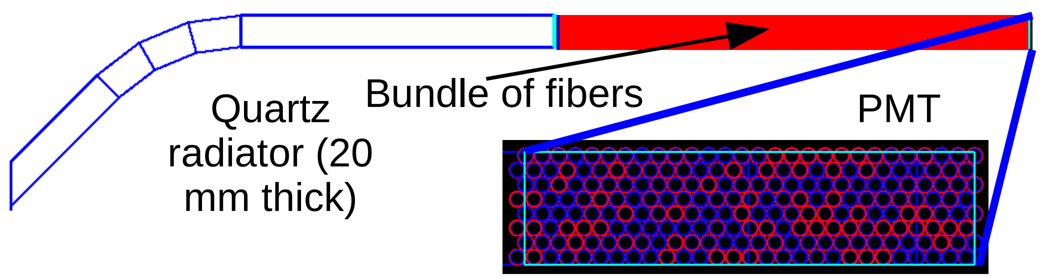

Main parameters to be optimized:

- Number of detected photons
- Should not be complicated (manufacturing problem)
- Compactness

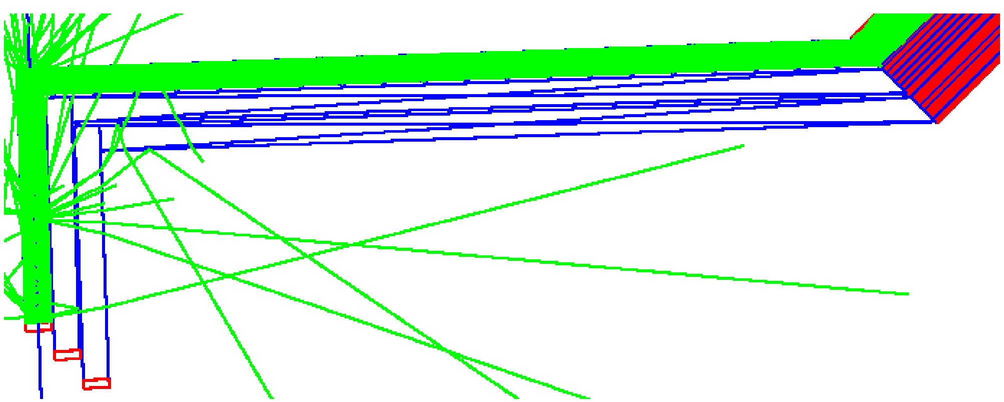

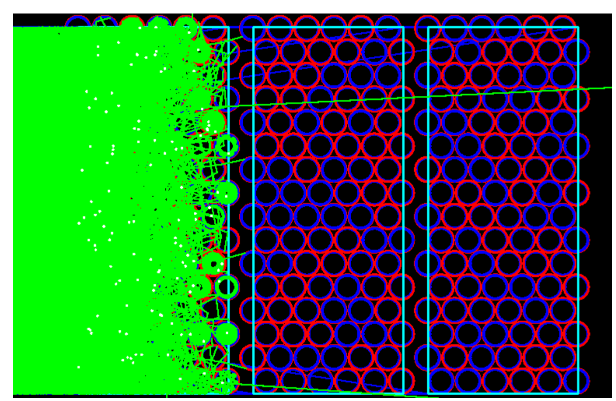

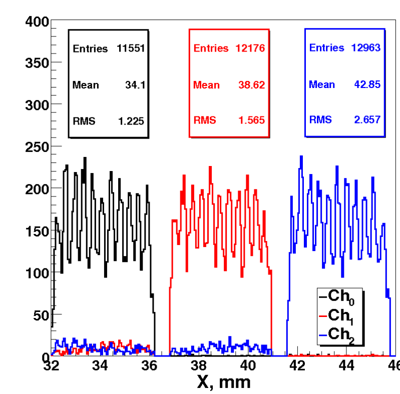

Optimal geometry!!!

Possible improvement of the CpFM

We obtain 15 % resolution (for 100 incoming electrons) with present geometry of the CpFM

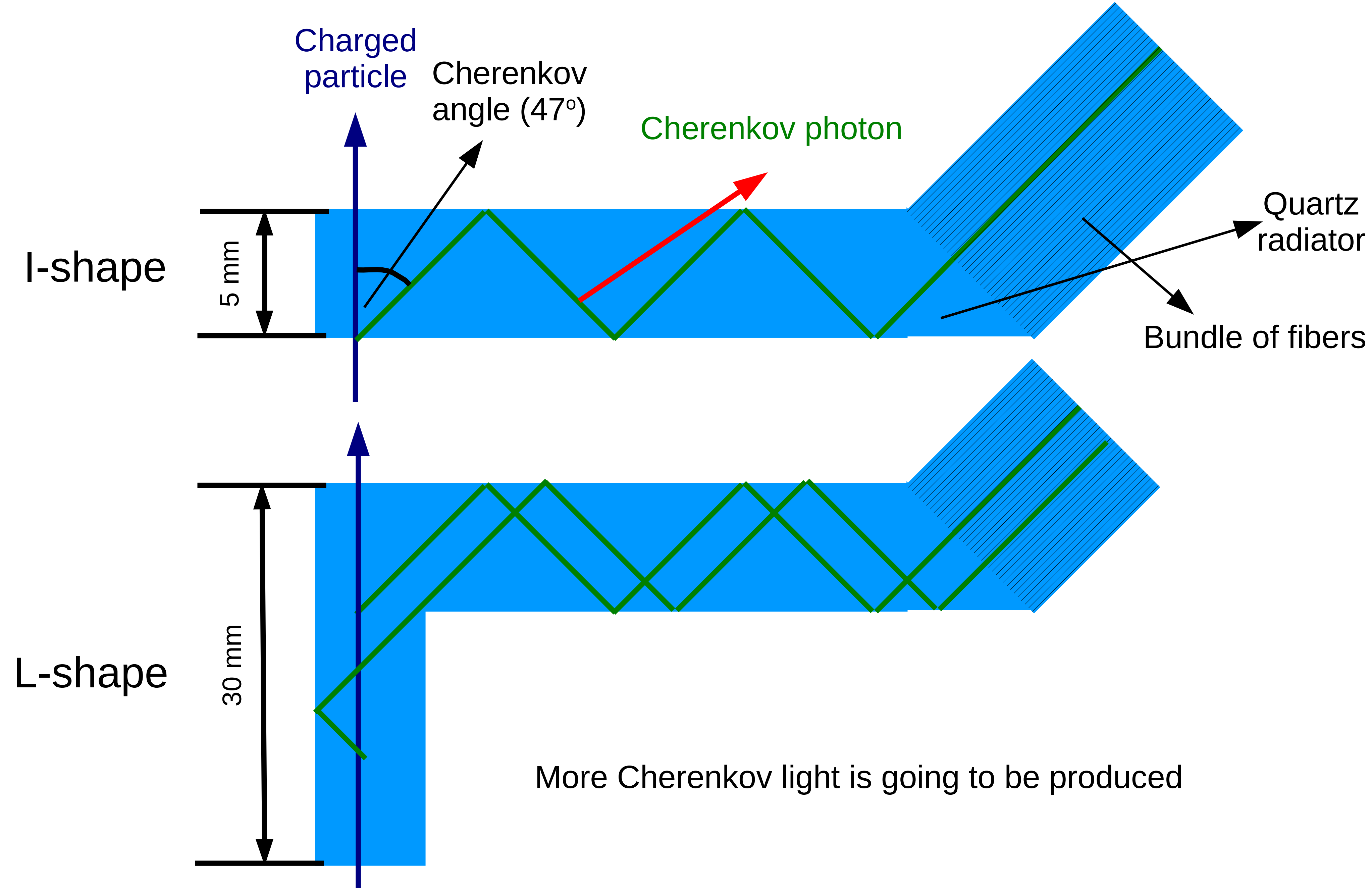

More Cherenkov light is going to be produced

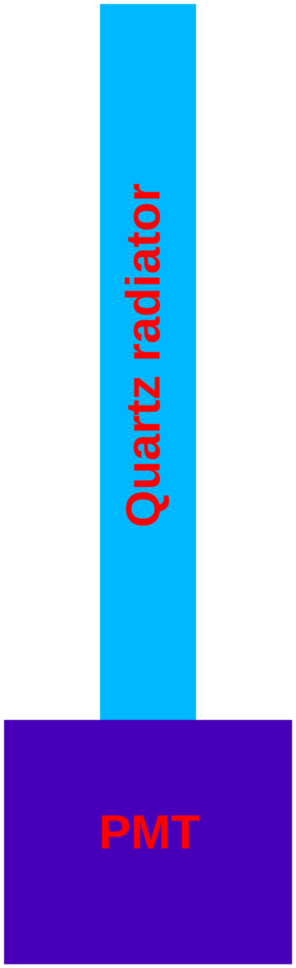
Quartz radiator
PMT


Quartz radiator
3.85 mm thick glass window
PMT